Human Molecular Genetics, 2015, Vol. 24, No. 2 **299–313**
doi:10.1093/hmg/ddu444
Advance Access published on September 3, 2014

Modeling type II collagenopathy skeletal dysplasia by directed conversion and induced pluripotent stem cells

Minoru Okada[1], Shiro Ikegawa[2], Miho Morioka[1], Akihiro Yamashita[1], Atsushi Saito[3], Hideaki Sawai[4], Jun Murotsuki[5], Hirofumi Ohashi[6], Toshio Okamoto[7], Gen Nishimura[8], Kazunori Imaizumi[3] and Noriyuki Tsumaki[1,9,*]

[1]Cell Induction and Regulation Field, Department of Cell Growth and Differentiation, Center for iPS Cell Research and Application, Kyoto University, Japan, [2]Laboratory of Bone and Joint Diseases, Center for Integrated Medicinal Sciences, RIKEN, Japan, [3]Department of Biochemistry, Graduate School of Biomedical & Health Sciences, University of Hiroshima, Japan, [4]Department of Obstetrics and Gynecology, Hyogo College of Medicine, Japan, [5]Maternal and Fetal Medicine, Miyagi Children's Hospital, Tohoku University School of Medicine, Japan, [6]Division of Medical Genetics, Saitama Children's Medical Center, Japan, [7]Department of Pediatrics, Asahikawa Medical University, Japan, [8]Department of Pediatric Imaging, Tokyo Metropolitan Children's Medical Center, Japan and [9]Japan Science and Technology Agency, CREST, Tokyo, Japan

Received January 10, 2014; Revised and Accepted August 26, 2014

Type II collagen is a major component of cartilage. Heterozygous mutations in the type II collagen gene (*COL2A1*) result in a group of skeletal dysplasias known as Type II collagenopathy (COL2pathy). The understanding of COL2pathy is limited by difficulties in obtaining live chondrocytes. In the present study, we converted COL2pathy patients' fibroblasts directly into induced chondrogenic (iChon) cells. The COL2pathy-iChon cells showed suppressed expression of *COL2A1* and significant apoptosis. A distended endoplasmic reticulum (ER) was detected, thus suggesting the adaptation of gene expression and cell death caused by excess ER stress. Chondrogenic supplementation adversely affected the chondrogenesis due to forced elevation of *COL2A1* expression, suggesting that the application of chondrogenic drugs would worsen the disease condition. The application of a chemical chaperone increased the secretion of type II collagen, and partially rescued COL2pathy-iChon cells from apoptosis, suggesting that molecular chaperons serve as therapeutic drug candidates. We next generated induced pluripotent stem cells from COL2pathy fibroblasts. Chondrogenically differentiated COL2pathy-iPS cells showed apoptosis and increased expression of ER stress-markers. Finally, we generated teratomas by transplanting COL2pathy iPS cells into immunodeficient mice. The cartilage in the teratomas showed accumulation of type II collagen within cells, a distended ER, and sparse matrix, recapitulating the patient's cartilage. These COL2pathy models will be useful for pathophysiological studies and drug screening.

INTRODUCTION

The type II collagen produced by chondrocytes is the major component of the cartilage extracellular matrix (1). The *COL2A1* gene encodes the type II collagen α1 chain. Supramolecular assembly of three α1 chains to form trimer molecules occurs in the endoplasmic reticulum (ER) lumen (2). The helical collagen molecules are trafficked via the Golgi network to the plasma membrane, and are then secreted into the extracellular space (3). There, the collagen proteins are assembled into dense fibrils.

Heterozygous mutations of *COL2A1* give rise to a spectrum of phenotypes predominantly affecting cartilage, collectively termed type II collagenopathies (COL2pathy) (4,5). Among them, achondrogenesis type II (ACGII) and hypochondrogenesis (HCG)

*To whom correspondence should be addressed at: Center for iPS Cell Research and Application, Kyoto University, 53 Kawahara-cho, Shogoin, Sakyo-ku, Kyoto 606-8507, Japan. Tel: +81 753667045; Fax: +81 753667047; Email: ntsumaki@cira.kyoto-u.ac.jp

© *The Author 2014. Published by Oxford University Press. All rights reserved.*
For Permissions, please email: journals.permissions@oup.com

Downloaded from http://hmg.oxfordjournals.org/ by guest on March 21, 2016

are lethal due to respiratory insufficiency, which is secondary to an abnormal chest wall skeleton. Individuals with HCG show a less severe phenotype compared with those with ACGII. Patients with spondyloperipheral dysplasia (SPD) live into adulthood and show a combination of platyspondyly and brachydactyly and early onset osteoarthritis (6).

Recent studies suggest that misfolded mutant collagens induce significant ER stress and trigger the ER stress signaling (7,8). Increased expression of ER stress markers, *Grp94* and *Chop*, is observed in mice with an ENU-induced missense mutation in *Col2a1* (9). Apoptosis was detected in the chondrocytes of mice harboring a *Col2a1* mutation (10). Mouse models have enormously contributed to the understanding of COL2pathy. However, the clinical translation of the findings may be diminished by the differences in size and locomotion between mice and humans. For example, the thickness of articular cartilage in the distal femur is 2.2 mm in humans, whereas it is 0.030 mm in mice (11). The volume density of chondrocytes in articular cartilage (chondrocytes + matrix) is about 2% in humans, whereas it is 15–40% in mice. The growth plate cartilage of humans and mice may also differ.

The emerging importance of the ER stress signaling in the pathology of COL2pathy offers the possibility of a new treatment strategy. If the misfolded protein load in the ER can be reduced to levels that can be managed by the cell, then the serious deleterious outcomes of an unresolved ER stress signaling, such as apoptosis, could be ameliorated (7). One promising approach uses small chemical chaperones, which can stabilize proteins in their native conformation and rescue mutant protein folding and/or trafficking defects, but such agents have never been tested for COL2pathy.

With the development of induced pluripotent stem (iPS) cells, cardiomyocytes, neurons and hepatocytes can be obtained by the differentiation of iPS cells derived from patients with various diseases (12–14). These cells, generated through iPS cells, may serve as a useful platform for exploring disease mechanisms and for drug screening. On the other hand, cells generated by directed conversion can also serve as a useful platform for exploring disease mechanisms, as neurons directly converted from skin fibroblasts from Alzheimer's disease patients recapitulated the pathophysiology of the disease (15). We previously developed a method to convert mouse dermal fibroblasts (MDFs) (16) and human dermal fibroblasts (HDFs) (17) directly into chondrogenic cells named induced chondrogenic (iChon) cells by transducing fibroblasts with two reprogramming factors (c-Myc and Klf4) and one chondrogenic factor (Sox9). Cells do not undergo a pluripotent state during direct induction of iChon cells from fibroblast culture by transduction of c-Myc, Klf4 and SOX9 (18). Human and mouse iChon cells express marker genes for chondrocytes but not fibroblasts and can form cartilage when transplanted into the subcutaneous spaces of immunodeficiency mice.

In order to provide live chondrocytes which recapitulate the features of COL2pathy, we generated chondrocytes from the HDFs of patients with COL2pathy using three different approaches: the induction of COL2pahty-iChon cells; the generation of COL2pathy-iPS cells, followed by chondrogenic differentiation and the generation of teratoma-containing cartilage from COL2pathy-iPS cells. These chondrocytes obtained through cellular reprogramming technologies suffered from abnormalities caused by excess ER stress and showed specific responses to reagents. The findings of our study may contribute to understanding the pathophysiology of the disease and to drug discovery for COL2pathy.

RESULTS

HDFs from patients with COL2pathy are normal

HDFs were obtained from two ACGII patients (ACGII-1 and ACGII-2), one HCG patient (HCG-1) and one SPD patient (SPD-1) (Supplementary Material, Table S1). The ACGII-2 patient showed an intermediate phenotype between ACGII and platyspondylic lethal skeletal dysplasia (PLSD)-Torrance type. Control HDFs from two different neonates were purchased (WT-1 and WT-2). A sequencing analysis of genomic DNA extracted from the patients' HDFs revealed heterozygous mutations in *COL2A1* in all patients (Supplementary Material, Fig. S1A). The ACGII-1 patient had a substitution mutation located at the acceptor site of exon 41. RT–PCR (Supplementary Material, Fig. S1B) and a sequencing analysis revealed the existence of multiple lengths of short mRNAs lacking various combinations of exons, thus resulting in inframe deletion by exon skipping. HDFs from patients with COL2pathy (COL2pathy-HDFs) showed morphologies and proliferation rates similar to those of control HDFs (WT-HDFs) (Supplementary Material, Fig. S1C and D). These results are consistent with the fact that neither WT-HDFs nor COL2pathy-HDFs express *COL2A1* (Supplementary Material, Fig. S1E). Accordingly, the transduction efficiencies did not differ between COL2pathy-HDFs and WT-HDFs (Supplementary Material, Fig. S1F).

Disturbed chondrocytic maturation of COL2-pathy iChon cells

We converted COL2pathy-HDFs into iChon cells and investigated whether COL2pathy-iChon cells can be used for disease modeling. Transduction of COL2pathy-HDFs with c-MYC, KLF4 and SOX9 produced a few Alcian blue-positive nodules, whereas the transduction of WT-HDFs produced substantial numbers of Alcian blue-positive nodules 21 days after transduction (Day 21) (Fig. 1A and Supplementary Material, Fig. S2A). The number of Alcian blue-positive nodules appeared to correlate with the severity of the diseases: ACGII-iChon cell culture showed a lower number of nodules than SPD-iChon cell culture. We next examined the iChon cells at earlier stages after transduction. By Day 7, WT-iChon cell colonies composed of polygonal-shaped cells had appeared (Fig. 1B, top panels; Supplementary Material, Movie S1). A polygonal shape is a characteristic of chondrocyte morphology, whereas HDFs are spindle-shaped. More than 90% of these polygonal cell colonies became condensed and subsequently multilayered, forming nodules by Day 13 (Fig. 1B, top panels; Supplementary Material, Fig. S2B and C). Approximately 95% of the nodules showed positive Alcian blue staining (Supplementary Material, Fig. S2B and C). The transduction of COL2pathy-HDFs also produced COL2pathy-iChon cell colonies composed of polygonal-shaped cells (Fig. 1B, bottom panels) with a comparable efficiency as the transduction of WT-HDFs (Supplementary Material, Fig. S2B, black bars). However, 80% of these

Downloaded from http://hmg.oxfordjournals.org/ by guest on March 21, 2016

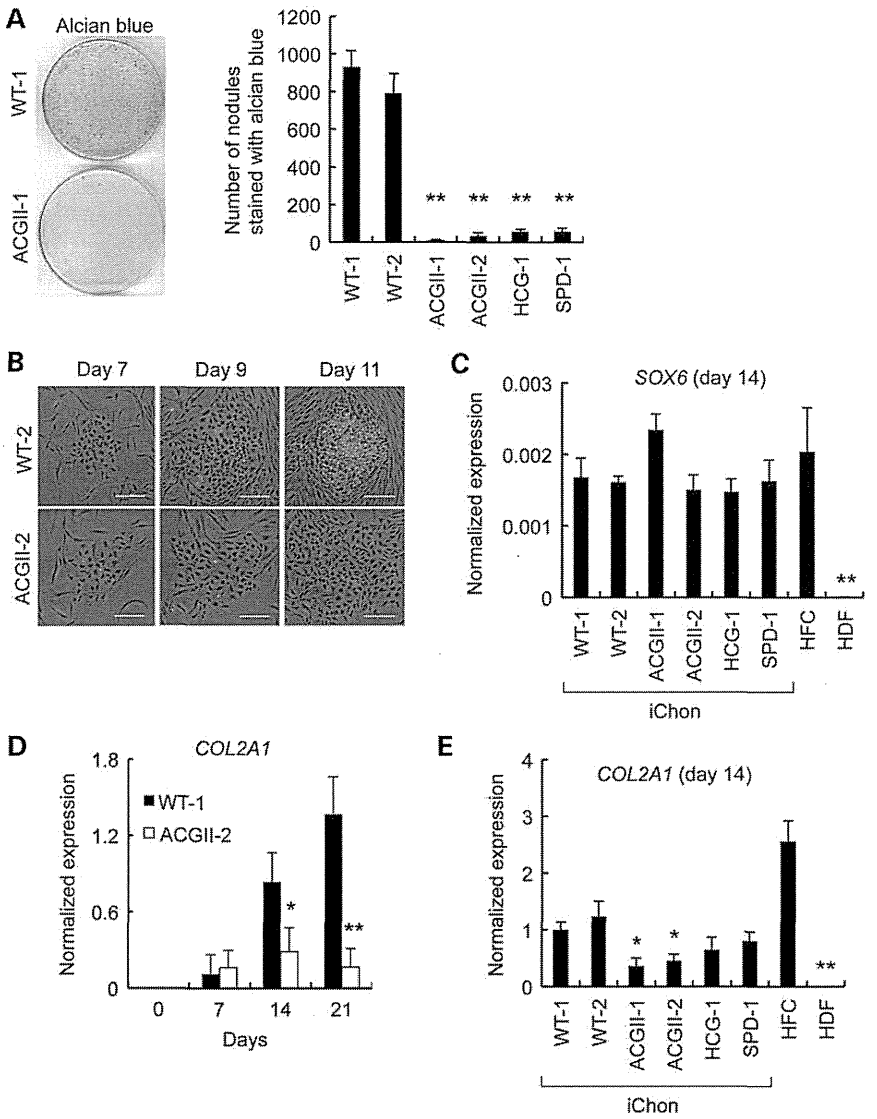

Figure 1. Disturbed chondrocytic maturation of COL2pathy-iChon cells. (**A**) After the transduction of HDFs with three factors (*c-MYC*, *KLF4* and *SOX9*), 1×10^5 cells were re-seeded into 100 mm dishes (Day 1). The dishes were stained with Alcian blue on Day 21. (Left) Representative images of the Alcian blue staining of iChon culture dishes from control WT-1-HDFs and patient ACGII-1-HDFs. (Right) The number of nodules positively stained with Alcian blue. $^{**}P < 0.01$ compared with WT-1 and WT-2 ($n = 3$). (**B**) Images of iChon cell colonies induced from WT-2-HDFs and ACGII-2-HDFs seven, nine and 11 days after transduction. Bars, 200 μm. (**C**) The iChon cell colonies were picked up on Day 14 and were subjected to a real-time RT–PCR expression analysis of *SOX6*. $^{**}P < 0.01$ compared with WT- and COL2pathy-iChon cells ($n = 3$). HFC, redifferentiated human fetal chondrocytes. (**D**) The iChon cell colonies were picked up at various intervals after transduction and were subjected to a real-time RT–PCR expression analysis for *COL2A1*. $^{*}P < 0.05$, $^{**}P < 0.01$ compared with WT-1 ($n = 3$). (**E**) The iChon cell colonies were picked up on Day 14 and were subjected to a real-time RT–PCR expression analysis for *COL2A1*. $^{*}P < 0.05$, $^{**}P < 0.01$ compared with WT-1 and WT-2 ($n = 3$).

COL2pathy-iChon cell colonies became neither condensed nor multilayered (Fig. 1B bottom panels; Supplementary Material, Fig. S2B), and were not stained with Alcian blue (Supplementary Material, Fig. S2B and C).

We picked up iChon cell colonies and subjected them to a real-time RT–PCR expression analysis. The expression levels of *SOX5* and *SOX6*, whose expression levels are induced by SOX9 (19), were similarly activated in WT-iChon cells and COL2pathy-iChon cells on Day 14 compared with those of HDFs (Fig. 1C and Supplementary Material, Fig. S2D). The expression levels of *SOX5* and *SOX6* in WT-iChon cells and COL2pathy-iChon cells were comparable to those of redifferentiated fetal chondrocytes (HFC), thus suggesting that chondrogenic commitment occurs in COL2pathy-iChon cells, as well as in WT-iChon cells. *COL2A1* transcription was initially activated similarly in WT-iChon cells and ACGII-2-iChon cells on Day 7 (Fig. 1D). The expression levels of *COL2A1* increased in WT-1-iChon cells as the time passed after transduction,

Downloaded from http://hmg.oxfordjournals.org/ by guest on March 21, 2016

suggesting that WT-1-iChon cells undergo chondrocytic maturation. On the other hand, the *COL2A1* expression in ACGII-2-iChon cells was suppressed as time passed on Days 14 and 21 (Fig. 1D and E). Furthermore, the expression levels of other cartilage matrix genes, such as *ACAN* and *COMP*, were also lower in COL2pathy-iChon cells than in control iChon cells on Day 14 (Supplementary Material, Fig. S2E). These results indicate that the chondrocytic maturation was disturbed in COL2pathy-iChon cells despite the activation of expression of *SOX5* and *SOX6*, which activate cartilage matrix gene expression in cooperation with SOX9 (20,21). These results suggest that an unknown mechanism(s) represses the expression of cartilage matrix genes in COL2pathy-iChon cells after the initial activation of type II collagen gene expression.

Decreased cell viabilities and increased ER stress in COL2pathy-iChon cells

We noticed that some COL2pathy-iChon cell colonies disappeared during culture (Supplementary Material, Fig. S3A and Supplementary Material, Movie S1). Approximately 20–30% of COL2pathy-iChon cell colonies disappeared by Day 18 (Supplementary Material, Fig. S3B). A growth curve analysis showed that the WT-1-iChon cells kept growing, whereas the numbers of ACGII-1- and HCG-1-iChon cells did not change or gradually decreased (Supplementary Material, Fig. S3C). The TUNEL assay revealed that more cells in COL2pathy-iChon cell colonies were TUNEL-positive than were the WT-iChon cell colonies around Day 15 (Fig. 2A). A transmission electron microscopic analysis revealed that the ER was distended in ACGII-2-iChon cells (Fig. 2B) on Day 14. The expression levels of *BIP* and *CHOP* were increased in COL2pathy-iChon cells on Day 18 (Fig. 2C), suggesting that there were increased ER stress signaling. The degree of increase was correlated with the severity of the patients' diseases. There are several pathways which transmit ER stress signals. *XBP1* splicing was detected in COL2pathy-iChon cells but not in WT-iChon cells on Day 17 (Fig. 2D), suggesting that the IRE1 pathway is involved in transmitting the ER stress. eIF2a was highly phosphorylated in the COL2pathy iChon cells compared with that in WT-iChon cells on Day 17 (Fig. 2E), suggesting that the PERK pathway is also involved in transmitting the ER stress. The expression levels of *GRP94* were increased in COL2pathy-iChon cells compared with those in WT-iChon cells on Day 18 (Fig. 2C), and cleaved ATF6 was detected in COL2pathy-iChon cells, but not in WT-iChon cells on Day 17 (Fig. 2F), suggesting that the ATF6 pathway is also involved in the transmission of ER stress. These results collectively suggest that COL2pathy-iChon cells have elevated ER stress and undergo apoptosis.

Ascorbic acid is a co-factor for prolyl hydroxylase and facilitates collagen triple helix formation, but the iChon cells were induced using DMEM culture medium with 10% FBS without ascorbic acid. To confirm that type II collagen trimers were formed in the iChon cells, we performed a western blot analysis using anti-type II collagen antibodies under the non-reducing condition (without dithiothreitol and 2-mercaptethanol) using samples obtained from the iChon cells on Day 19. We detected type II collagen molecules with a size between 268 and 460 kDa in the lysates from COL2pathy-iChon cells, but not in the lysates from WT-iChon cells (Fig. 2G, left top panel). On the other hand, we detected type II collagen molecules with a size between 268 and 460 kDa in the supernatant from WT-iChon cell cultures, but it was minimally present in the supernatant from COL2pathy-iChon cell cultures (Fig. 2G, right panel). These results suggest that type II collagens were folded correctly in both WT- and COL2pathy-iChon cells, even when they were cultured in the absence of ascorbic acid. The folded type II collagen molecules were immediately secreted from WT-iChon cells, whereas misfolded type II collagen trimers were probably retained in the COL2pathy-iChon cells. These results collectively suggest that the excess ER stress in the COL2pahty-iChon cells is likely associated with the misfolding of type II collagen.

To confirm that the misfolding of mutant proteins is responsible for the abnormalities of the COL2pathy-iChon cells, we induced WT- and COL2pahty-iChon cells in the presence of ascorbic acid. We added ascorbic acid to the medium from Day 6 to Day 17 during the induction of WT- and COL2pathy-iChon cells, and subjected them to an analysis on Day 17. The application of ascorbic acid did not significantly change the number of Alcian blue-positive nodules in the WT-iChon cell culture, but did significantly decrease the numbers of Alcian blue-positive nodules in the ACGII-1- and HCG-1-iChon cell cultures (Fig. 3A). The addition of ascorbic acid increased the expression levels of ER stress markers; *BIP*, *GFP94* and *CHOP*, in the COL2pathy-iChon cells (Fig. 3B). The presence of ascorbic acid in the culture did not affect the *XBP1* splicing in either WT- or COL2pathy-iChon cells (Fig. 3C). The administration of ascorbic acid increased the amount of phosphorylated eIF2a (Fig. 3D) and cleaved ATF6 (Fig. 3E) in the COL2pathy-iChon cells. Therefore, the presence of ascorbic acid enhanced the abnormalities and increased the activation of ER stress pathways, including the PERK pathway and the ATF6 pathway, in COL2pathy iChon cells, supporting the idea that the misfolding of mutant proteins is responsible for the abnormalities of COL2pathy-iChon cells.

To examine how type II collagen molecules became degraded in the ACGII-iChon cells, we generated iChon cells in the presence of ascorbic acid, treated them with MG132 (a proteasome inhibitor) or bafilomycin A1 (a lysosome inhibitor), collected cell lysates and subjected them to a western blot analysis using an anti-type II collagen antibody (Fig. 3F). The addition of bafilomycin A1 increased the amount of type II collagen, whereas the addition of MG132 did not, suggesting that there is lysosomal degradation of type II collagen.

Chondrogenic supplementation adversely affects COL2pathy-iChon cells

We analyzed how chondrogenic stimulation with BMP2 and TGFβ1 (B + T) affects COL2pathy-iChon cells (Fig. 4A). The addition of B + T to WT-iChon cell culture slightly increased the numbers of Alcian blue-positive nodules due to the chondrogenic effects of B + T (Fig. 4A and Supplementary Material, Fig. S4A). On the other hand, the addition of B + T to COL2pathy-iChon cell culture decreased the numbers of Alcian blue-positive nodules. The degree of decrease correlated with the severity of the original patient diseases.

We picked up and reseeded iChon colonies, and continued their cultivation in the presence or absence of B + T, for the

Downloaded from http://hmg.oxfordjournals.org/ by guest on March 21, 2016

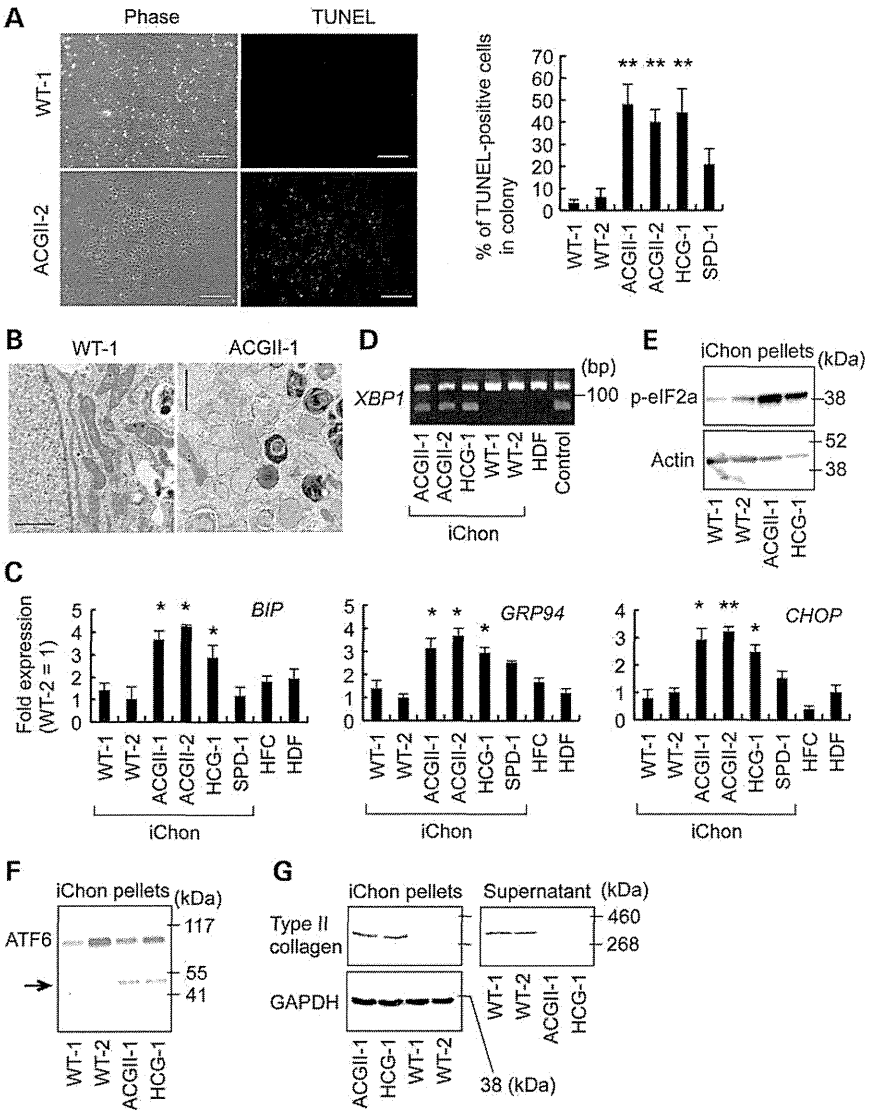

Figure 2. An analysis of the apoptosis and ER stress in COL2pathy-iChon cells. (**A**) (Top) TUNEL assay of iChon cell colonies on Day 14. Bars, 200 μm. (Bottom) The ratio of the number of TUNEL-positive cells to the total number of cells within each iChon cell colony was calculated around Day 15. $^{*}P < 0.05$, $^{**}P < 0.01$ compared with WT-1 and WT-2 ($n = 5$). (**B**) A transmission electron microscopic analysis of WT-1- and ACGII-2-iChon cells on Day 14. Bars, 1 μm. (**C**) The iChon cell colonies were picked up on Day 18 and were subjected to a real-time RT–PCR expression analysis of ER stress markers, *BIP*, *GRP94* and *CHOP*. HFC, redifferentiated human fetal chondrocytes. $^{*}P < 0.05$, $^{**}P < 0.01$ compared with WT-1 and WT-2 ($n = 3$). (**D**) The iChon cell colonies were picked up on Day 17 and were subjected to a RT–PCR analysis of the splice variants of *XBP1*. As a control, HDFs treated with 10 μg/ml tunicamycin for 4 h were used. (**E**) The iChon cell colonies were picked up on Day 17 and were subjected to a western blot analysis of the phospho-eIF2a expression in iChon cells. (**F**) The iChon cell colonies were picked up on Day 17 and were subjected to a western blot analysis of the ATF6 expression in iChon cells. The arrow shows cleaved ATF6. (**G**) The iChon cell colonies were picked up on Day 17 and transferred to a well of a six-well plate. The medium was changed on Day 18. The supernatants and cells were collected on Day 19 and subjected to a western blot analysis of the type II collagen expression under the non-reducing condition.

expression analysis (Fig. 4B). The WT-iChon cell colonies stayed alive, regardless of the presence or absence of B + T (Supplementary Material, Fig. S4B). On the other hand, 10% of ACGII-2 iChon cell colonies died in the absence of B + T (Fig. 4C). The addition of B + T caused the death of half of ACGII-2-iChon cell colonies (Fig. 4C). A real-time RT–PCR analysis revealed that the addition of B + T increased the expression of *COL2A1* in both WT-1- and ACGII-2-iChon cell colonies (Supplementary Material, Fig. S4C and Fig. 4D). The addition of ascorbic acid did not affect the viability of WT-iChon cells, but did decrease the viabilities of ACGII-iChon cells both in the presence and absence of B + T (Supplementary Material, Fig. S4D). Together, these findings suggest that the addition of B + T forced COL2pathy-iChon cells to express

Downloaded from http://hmg.oxfordjournals.org/ by guest on March 21, 2016

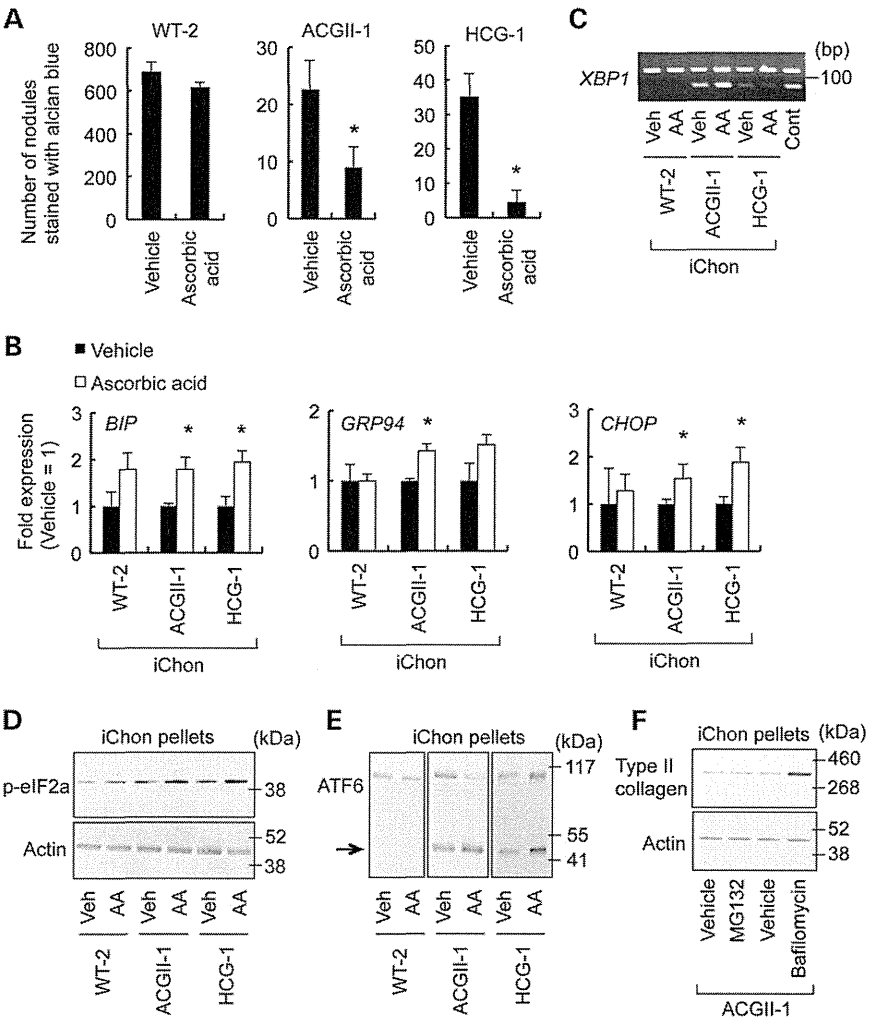

Figure 3. The effects of ascorbic acid on the abnormalities in COL2pathy-iChon cells. WT- and COL2pathy-iChon cells were induced in the presence and absence of ascorbic acid from Day 6 to Day 17. The iChon cell cultures were stained with Alcian blue on Day 17 (**A**). The iChon cell colonies were picked up for the RT-PCR and Western blot analyses on Day 17 (**B**–**F**). (A) After the transduction of HDFs with three factors (*c-MYC*, *KLF4* and *SOX9*), 1×10^5 cells were re-seeded onto 100 mm dishes (Day 1) and cultured in the presence or absence of ascorbic acid. The dishes were stained with Alcian blue on Day 17. The number of nodules positively stained with Alcian blue was counted. $^*P < 0.05$, $^{**}P < 0.01$ ($n = 3$). (B) The results of the real-time RT–PCR expression analysis of ER stress markers; *BIP*, *GRP94* and *CHOP*. HFC, redifferentiated human fetal chondrocytes. $^*P < 0.05$, $^{**}P < 0.01$ compared with WT-1 and WT-2 ($n = 3$). (C) The results of the RT–PCR analysis of the splice variants of *XBP1* on Day 17. HDFs treated with 10 μg/ml tunicamycin for 4 h were used as a control. (D) The results of the western blot analysis of the phospho-eIF2a expression in iChon cells. (E) The results of the western blot analysis of the ATF6 expression in iChon cells. The arrow show cleaved ATF6. (F) The results of the western blot analysis of type II collagen in iChon cells in the presence of a proteasome inhibitor (MG132) or lysosome inhibitor (bafilomycin A1).

COL2A1, including mutant *COL2A1*, thus resulting in an increased amount of misfolded protein and ER stress, which eventually led to the death of iChon cells and reduced the numbers of Alcian blue-positive nodules.

TMAO, a chemical chaperone, improved secretion of type II collagen and partially reduced apoptosis in COL2pathy-iChon cells

We then examined whether a chemical chaperone known to regulate protein folding could rescue the COL2pathy-iChon cells from abnormalities. The addition of trimethylamine N-oxide (TMAO) partially, but significantly, decreased the degree of apoptosis in COL2pathy-iChon cells (Fig. 4E). The addition of TMAO increased the amount of extracellularly secreted type II collagen (Fig. 4F), increased the Alcian blue staining (Supplementary Material, Fig. S4E) and reduced the expression levels of ER stress-related markers, *BIP*, *CHOP*, *GRP94*, *p58IPK* and *ERdj4* (Fig. 4G and Supplementary Material, Fig. S4F), in COL2-pathy iChon cell culture. These results suggest that TMAO may stabilize the misfolded type II collagen molecules, leading to the improved secretion and accumulation of the extracellular molecules and rescuing cells from apoptosis in COL2pathy-iChon cell culture.

Downloaded from http://hmg.oxfordjournals.org/ by guest on March 21, 2016

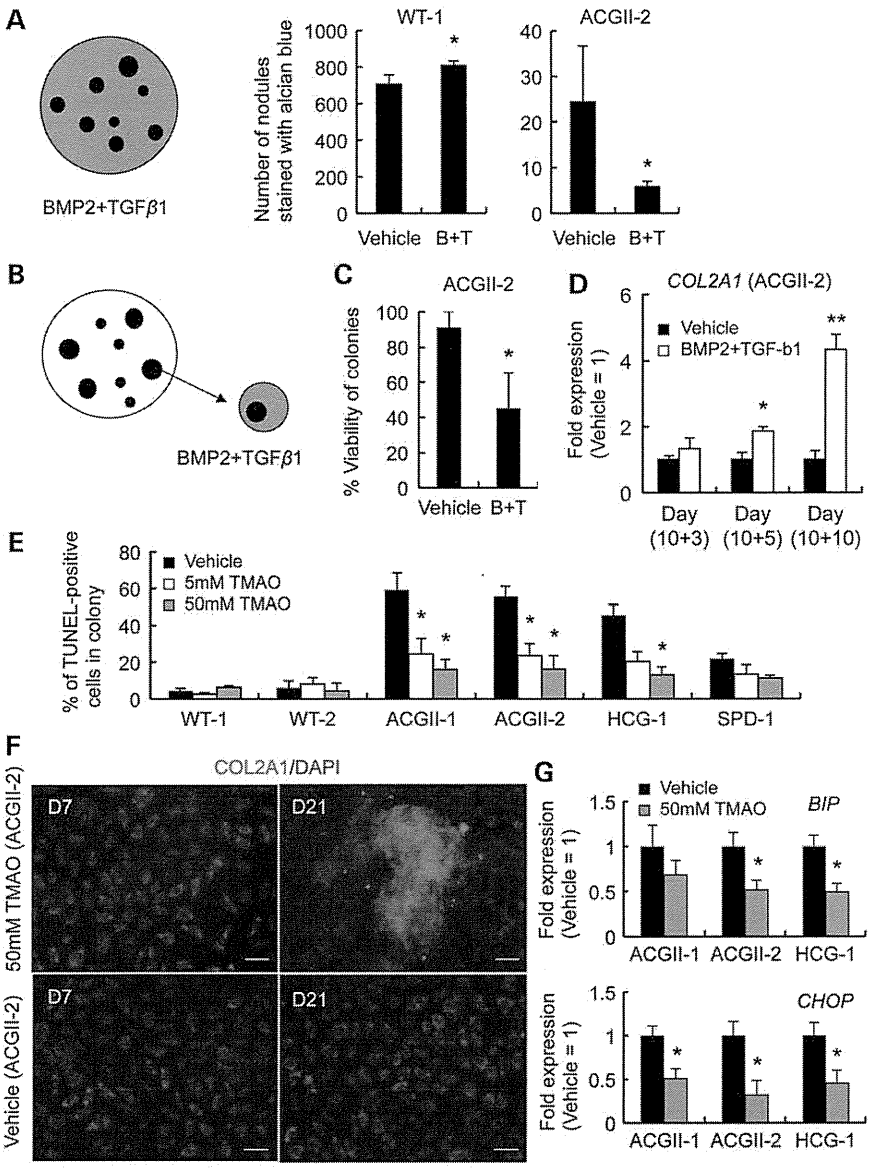

Figure 4. Effects of BMP2/TGFβ1 and chemical chaperones on COL2pathy-iChon cells. In (**A**) and (**B**), the black dots indicate iChon colonies and grey areas represent medium containing BMP2 and TGFβ1. B + T, presence of BMP2 and TGFβ1. (A) After the transduction of HDFs with three factors (*c-MYC*, *KLF4* and *SOX9*), 1×10^5 cells were re-seeded into 100 mm dishes (Day 1). BMP2 and TGFβ1 were added to the medium from Day 10 to Day 18, and dishes were subjected to Alcian blue staining on Day 18. The numbers of Alcian-blue positive nodules were counted. $^*P < 0.05$ compared with dishes in the absence of BMP2 and TGFβ1 (Vehicle) ($n = 3$). (B) A schematic representation of the experiments in (**C**) and (**D**). We picked up iChon cell colonies on Day 10, replated them into individual wells and cultured them in the presence or absence of BMP2 and TGFβ1. (C) The ratio of the number of wells in which iChon cells survived for 15 days to the number of wells that initially had ACGII-2-iChon cell colonies. A total of 10–12 ACGII-2-iChon cell colonies were picked up and individually replated into new wells for each experiment. $^*P < 0.05$ compared with the ratio in the absence of BMP2 and TGFβ1 (Vehicle) ($n = 3$). (D) The results of a real-time RT–PCR expression analysis of *COL2A1* in ACGII-2-iChon cells cultured in the presence or absence of BMP2 and TGFβ1 for 3, 5 and 10 days. $^*P < 0.05$, $^{**}P < 0.01$ compared with iChon colonies in the absence of BMP2 and TGFβ1 (Vehicle) ($n = 3$). (**E**) The effects of TMAO on the COL2pathy-iChon cells. TMAO was added to the cultures at a final concentration of 5 or 50 mM from Day 7 to Day 18. The iChon cell colonies were subjected to a TUNEL staining analysis on Day 18. The ratios of the number of TUNEL-positive cells to the number of total cells in each iChon colony are shown. $^*P < 0.05$ compared with iChon colonies cultured in the absence of TMAO (Vehicle) ($n = 5$). (**F**) Immunocytochemical staining of ACGII-iChon cell nodules for type II collagen in the presence or absence of TMAO on Days 7, 14 and 21. Bars, 100 μm. (**G**) The COL2pathy-iChon cells were cultured in the presence or absence of TMAO. iChon colonies were picked up on Day 18 and were subjected to a real-time RT–PCR expression analysis of ER stress markers, *BIP* and *CHOP*. $^*P < 0.05$ compared with WT-1 and WT-2 ($n = 3$).

Downloaded from http://hmg.oxfordjournals.org/ by guest on March 21, 2016

Generation of ACGII- and HCG-specific iPS cells

Another approach to modeling COL2pathy is the generation of iPS cells, followed by differentiation of these cells toward chondrocytes. This approach takes time, but has an advantage in that it can provide an almost unlimited supply of materials, because once iPS cells are established, they can be expanded indefinitely.

We next generated iPS cells from the HDFs from two controls (WT-1 and WT-2), two ACGII patients (ACGII-1 and ACGII-2) and one HCG patient (HCG-1). We established three independent iPS cell lines (#) for each individual (Supplementary Material, Table S2). There were no obvious differences in the induction efficiency, cell morphologies (Fig. 5A), expression levels of pluripotent markers (Fig. 5B and C) or pluripotency as indicated by teratoma formation (Fig. 5D), between the WT-iPS cells, ACGII-iPS and HCG-iPS cells (Supplementary Material, Table S2). The karyotypes of the WT-iPS and ACGII-iPS cells examined were normal (Fig. 5E and Supplementary Material, Table S2). The ACGII-iPS and HCG-iPS cells were indistinguishable from control iPS cells, which was consistent with the fact that type II collagen is expressed by neither HDFs (Supplementary Material, Fig. S1E) nor the resulting iPS cells (Fig. 5F), and is unlikely to be expressed during the process of inducing the iPS cells.

In vitro differentiation of ACGII-iPS and HCG-iPS cells toward chondrocytes

We generated chondrocytes from iPS cells by following the previously described method (23), with some modifications. The targeted differentiation of iPS cells toward prochondrogenic cells was performed by serially adding combinations of growth factors for 14 days (Supplementary Material, Fig. S5A). The expression of pluripotency markers (*OCT3/4* and *NANOG*) decreased, and the expression of mesoendodermal markers (*T* and *KDR*) transiently increased, in the WT-iPS, ACGII-iPS and HCG-iPS cells that underwent differentiation (Supplementary Material, Fig. S5B). On Day 14, differentiated WT-iPS cells, ACGII-iPS and HCG-iPS cells were multilayered (Fig. 6A). We then scraped the cells and subjected them to pellet culture for chondrogenic maturation. The expression levels of chondrocytic markers increased gradually in the differentiated WT-iPS cells, whereas the level increased slightly on Days 14 and 28 and decreased on Day 42 in the differentiated ACGII-iPS and HCG-iPS cells (Fig. 6B). We then analyzed the pellets histologically. Cells were embedded in matrix, which was positively stained with safranin O, in the pellets generated from differentiated WT-iPS cells, whereas the pellets of differentiated ACGII-iPS cells were not stained with safranin O (Fig. 6C and Supplementary Material, Fig. S6). The cells in the pellets of differentiated ACGII-iPS cells underwent apoptosis, as indicated by their expression of cleaved caspase-3 and positive TUNEL staining (Fig. 6C). The expression of ER stress markers in differentiated ACGII-iPS and HCG-iPS cells was significantly elevated compared with that in differentiated WT-iPS cells on Day 42 (Fig. 6D and Supplementary Material, Fig. S5C). Furthermore, TMAO reduced the expression of ER stress markers (Supplementary Material, Fig. S5D). These results indicate that the chondrogenic differentiation of ACGII-iPS and HCG-iPS cells causes ER stress and apoptosis.

To determine which types of chondrocytic cells were generated by these two methods (induction of iChon cells and chondrogenic differentiation of iPS cells), we analyzed the expression of marker genes for growth plate cartilage and articular cartilage (Supplementary Material, Fig. S7). The WT-iChon cells and chondrogenically differentiated WT-iPS cells expressed markers for articular cartilage (*PRG4* and *CILP*), but not markers for hypertrophic chondrocytes in the growth plate (*COL10A1* and *MMP13*). These results suggest that the iChon cells and chondrogenically differentiated iPS cells may have the characteristics of articular chondrocytes or epiphyseal proliferative chondrocytes in primordial cartilage.

Modeling of ACGII-cartilage in teratomas in immunodeficient mice

We next examined the cartilage in teratomas formed by the transplantation of iPS cells into immunodeficient mice. A histological analysis of the teratomas revealed that cartilage tended to be smaller, and that the extracellular matrix was thinner and more weakly stained with safranin O in the teratomas formed by ACGII-iPS cells compared with the cartilage in teratomas formed by WT-iPS cells (Fig. 7A). The chondrocytes were large in the teratomas formed by ACGII-iPS cells. These histological findings recapitulate the findings of cartilage obtained from ACGII patients at the time of autopsy (24,25).

An immunohistochemical analysis showed that type II collagen existed abundantly in the extracellular matrix, but not inside of cells, in the cartilage in the teratomas formed by WT-iPS cells (Fig. 7B, top panels). On the other hand, type II collagen existed in a thin matrix in a reduced amount, and existed within the cells, in the cartilage in the teratomas formed by ACGII-iPS cells (Fig. 7B, bottom panels). The type II collagen detected within these cells may correspond to the accumulation of misfolded type II collagen in the rER. Cartilage containing such chondrocytes bearing type II collagen within the cells were absent in the immunohistological sections of teratomas formed by control iPS cells (Fig. 7C).

An electron microscopic analysis revealed a distended rER in the chondrocytes in the teratomas formed by ACGII-iPS cells (Fig. 7D). The extracellular matrix showed reduced densities of collagen fibrils (Fig. 7E). These results collectively demonstrate that COL2pathy-specific teratomas contain cartilage which recapitulates the cartilage tissue in patients with COL2pathy.

DISCUSSION

We herein performed disease modeling for type II collagenopathies using three approaches: (i) directed conversion from patient-specific HDFs to iChon cells; (ii) the generation of iPS cells from patient-specific HDFs, followed by the differentiation of these cells toward chondrocytes *in vitro* and (iii) the generation of iPS cells, followed by the formation of teratomas containing cartilage in mice. Using these approaches, the expected pathological features, such as elevated expression of ER stress markers, apoptosis, the retention of type II collagen within cells and abnormal ultrastructure of the extracellular matrix, were recapitulated. In addition, the severity of diseases tended to correlate with degrees of abnormalities in the COL2pathy-

Downloaded from http://hmg.oxfordjournals.org/ by guest on March 21, 2016

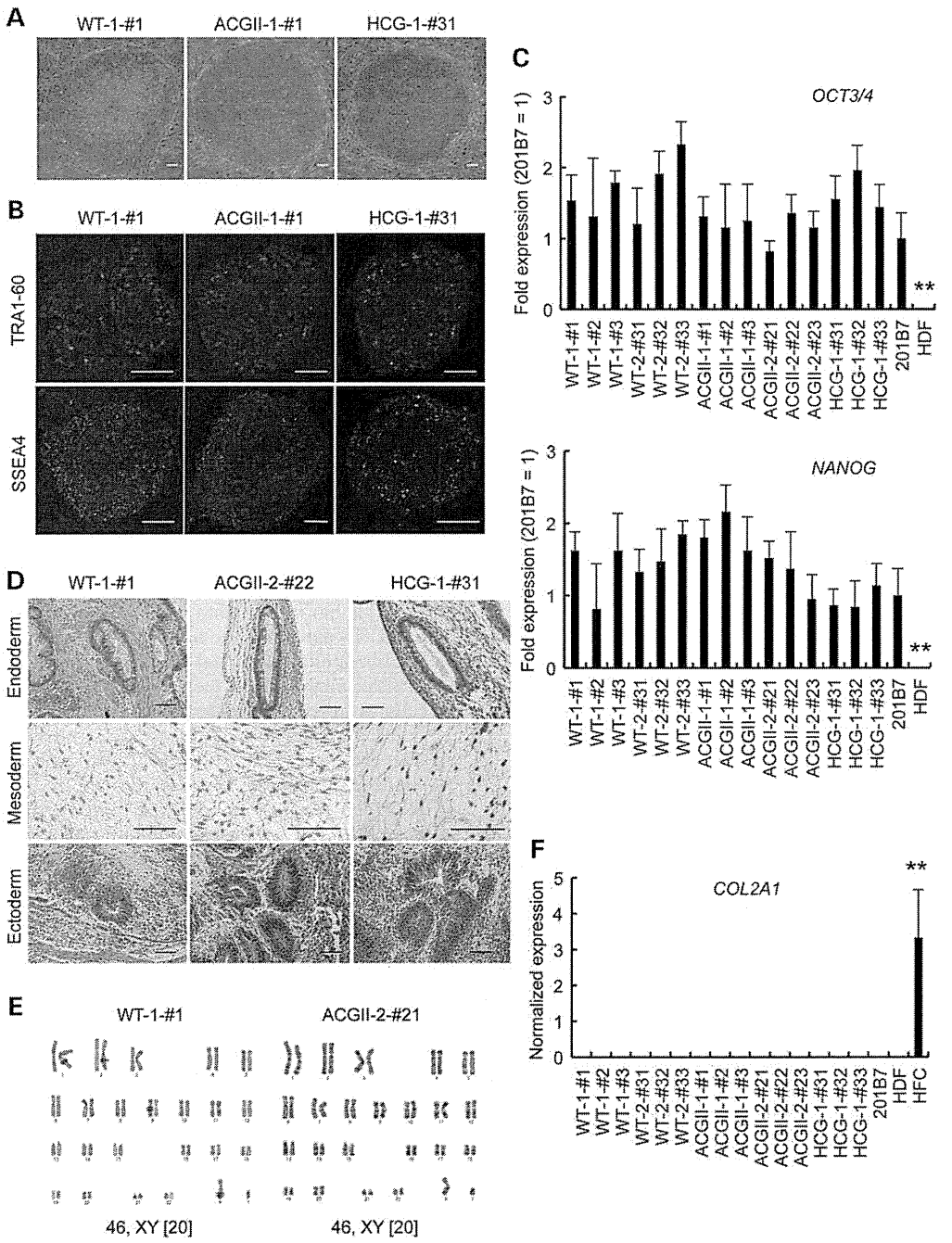

Figure 5. Generation of iPS cells from HDFs from two control neonates (WT-1 and WT-2), HDFs from two ACGII patients (ACGII-1 and ACGII-2) and HDFs from one HCG patient (HCG-1). Three independent iPS cell lines (#) were established for each individual. (**A**) The morphology of iPS cells generated from WT-1-HDFs, ACGII-1-HDFs and HCG-1-HDFs. There were not obvious differences in the cell morphologies between WT-iPS cells and ACGII-iPS cells. Bars, 50 μm. (**B**) The immunocytochemical analysis. WT-1-#1-iPS cells, ACGII-1-#1-iPS cells and HCG-1-#31-iPS cells expressed TRA1-60 and SSEA4. Bars, 100 μm. (**C**) The results of a real-time RT–PCR expression analysis of *OCT3/4* and *NANOG* in iPS cell lines. The previously reported iPS cell clone, 201B7 (22), was used as a positive control. There were no significant differences in the expression levels among the WT-iPS cells, ACGII-iPS cells and HCG-iPS cells. ($n = 3$). $^{**}P < 0.01$ compared with iPS cell lines. (**D**) The results of the teratoma formation assay. iPS cells were injected into testicular capsules. The masses formed at the injected sites were recovered 6–8 weeks after injection, and were subjected to a histological analysis. Teratomas containing tissues from all three germ layers were formed by the injection of WT-1-#1 iPS cells, ACGII-2-#22 iPS cells and HCG-#31-iPS cells. Hematoxylin and eosin staining. Bars, 100 μm. (**E**) The results of a karyotype analysis of iPS cell lines (WT-1-#1 and ACGII-2-#21). A total of 20 cells for each cell line was examined. The numbers in brackets indicate the number of cells showing the karyotype presented. All 20 cells in both cell lines showed a normal 46XY karyotype. (**F**) The results of a real-time RT–PCR expression analysis of *COL2A1* expression in iPS cell lines. HFC, redifferentiated human fetal chondrocytes. ($n = 3$). $^{**}P < 0.01$ compared with iPS cell lines.

Downloaded from http://hmg.oxfordjournals.org/ by guest on March 21, 2016

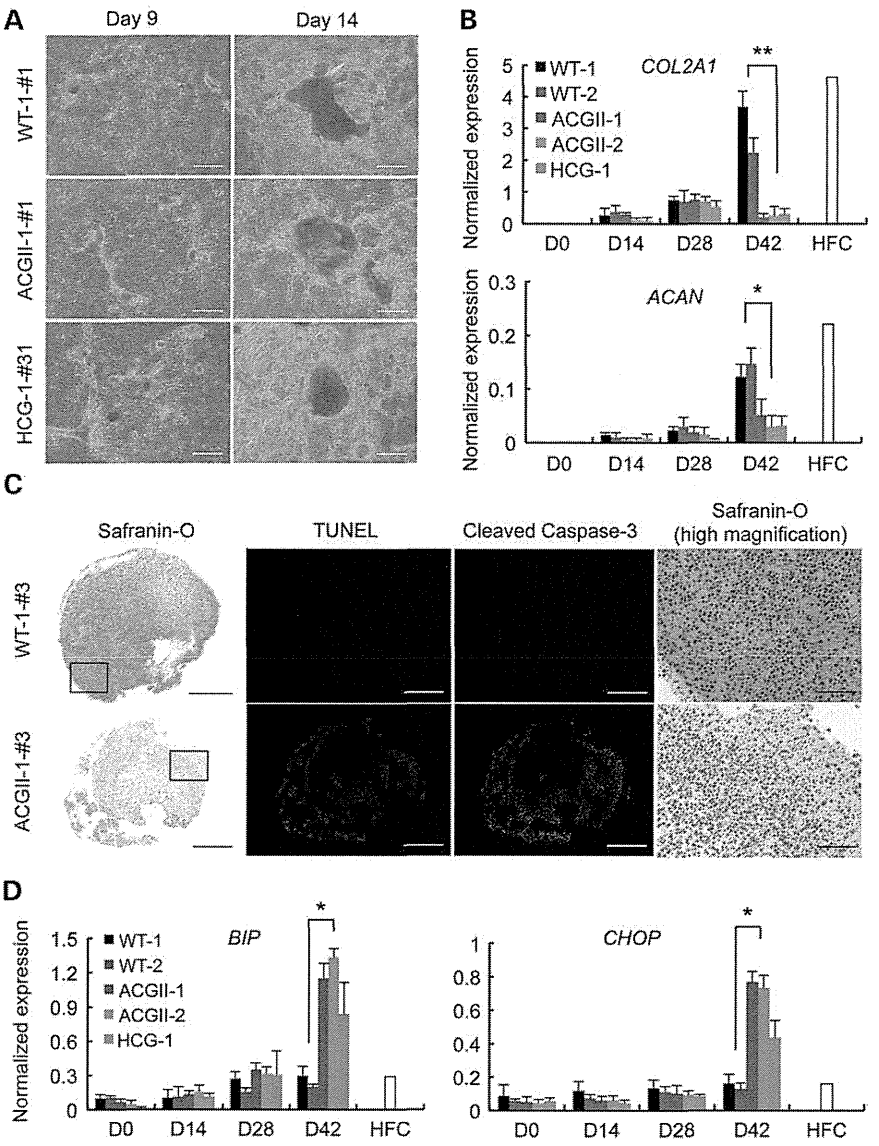

Figure 6. Chondrogenic differentiation of COL2pathy-iPS cells. (**A**) iPS cells were differentiated toward chondrocytes following the protocol shown in Supplementary Material, Figure S5A. A phase contrast image of the cultures on Days 9 and 14. Bars, 200 μm. (**B**) The results of the expression analysis for chondrogenic markers. Cells or pellets were harvested on Days 0, 14, 28 and 42, and were subjected to a real-time RT–PCR expression analysis. $^{*}P < 0.05$, $^{**}P < 0.01$ compared with WT-1 and WT-2 ($n = 3$). HFC, redifferentiated human fetal chondrocytes. (**C**) The histological analysis of the pellet culture of chondrogenically differentiated ACGII-iPS cells. Pellets were subjected to an analysis on Day 42. Sections were stained with safranin O, immunostained with anti-cleaved caspase-3 and subjected to the TUNEL assay. Magnified images of the boxed region in the left panels are shown in the right panels. The bars in the left and center panels, 500 μm; bars in the right panels, 50 μm. (**D**) The results of the expression analysis for ER stress markers. Cells or pellets were harvested on Days 0, 14, 28 and 42, and were subjected to a real-time RT–PCR expression analysis. $^{**}P < 0.01$ compared with WT-1 and WT-2 ($n = 3$). HFC, redifferentiated human fetal chondrocytes.

iChon cells. These results suggest that the models presented in this study can provide a useful platform for investigating the pathomechanisms of and drug screening for COL2pathy. In fact, we investigated the cellular response of the model to reagents which increase ER stress (BMP and TGFβ) or reduce ER stress (TMAO), which provided insights into the pathomechanisms underlying COL2pathy and some information for drug discovery.

The cellular consequences of ER stress signaling are context-dependent, and range from adaptation to cell death, depending on the levels of ER stress signaling (8). By analyzing iChon cell models of COL2pathy, we discovered several findings that may contribute to understanding the pathomechanics of COL2-pathy. The COL2pathy-iChon cells are chondrogenically committed, because the levels of *SOX5* and *SOX6* expression in the COL2pathy-iChon cells were similar to those in control iChon

Downloaded from http://hmg.oxfordjournals.org/ by guest on March 21, 2016

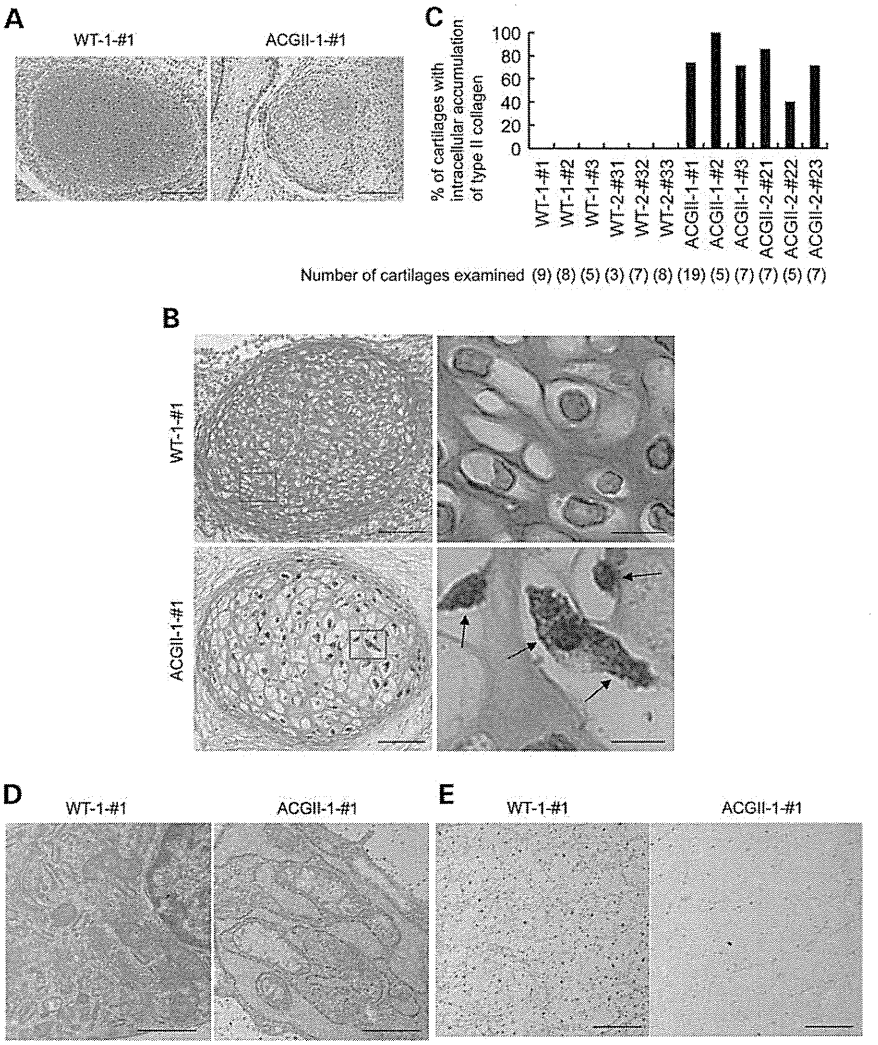

Figure 7. Examination of the cartilage formed in teratomas. (**A**) Safranin O-fast green-iron hematoxylin staining. The extracellular matrix was intensely stained with safranin O in the cartilage in teratomas generated by the injection of WT-1-#1-iPS cells. The extracellular matrix was weakly stained with safranin O in the cartilage in teratomas generated by injection of ACGII-1-#1-iPS cells. Bars, 200 μm. (**B**) Immunohistochemistry for type II collagen in the cartilage in teratomas generated by injection of WT-1-#1-iPS cells and ACGII-1-#1-iPS cells. The boxed regions in the left panels are magnified and shown on the right. Note the intense signal (arrows) within the chondrocytes in the bottom right panel. Bars, 100 μm (left), 20 μm (right). (**C**) The number of cartilage tissues which contained chondrocytes bearing type II collagen within cells was divided by the total number of cartilage tissues on the immunohistological sections of teratomas. The total number of cartilage tissues is indicated at the bottom. (**D**) The results of a transmission electron microscopic analysis of chondrocytes. Note the distended rER in chondrocytes in the cartilage in teratomas generated by injection of ACGII-1-#1-iPS cells. Bars, 1 μm. (**E**) The results of a transmission electron microscopic analysis of the extracellular matrix. Note the sparse collagen fibrils in the extracellular matrix in the cartilage in teratomas generated by injection of ACGII-1-#1-iPS cells. Bars, 1 μm.

cells and were comparable to those in HFCs on Day 14 (Fig. 1C and Supplementary Material, Fig. S2D). The expression levels of *COL2A1* gradually increased during the maturation of iChon cells (Fig. 1D), probably resulting in an accumulation of mutant *COL2A1* and unfolded protein in the rER in COL2pathy-iChon cells (Fig. 2B). This caused ER stress signaling (Fig. 2C–F). When the ER stress is moderate, ER stress signaling may result in adaptations to reduce the expression of *COL2A1* (Fig. 1D and E) and other cartilage matrix genes (Supplementary Material, Fig. S2E) to decrease the amount of misfolded protein. When ER stress is further increased due to the maturation of iChon cells, the increased ER stress signaling may induce cell death (Fig. 2A and Supplementary Material, Movie S1).

Controlling *COL2A1* expression is important in the development of the disease phenotype

We found that the treatment of COL2pathy-iChon cells with BMP2 and TGFβ1 inhibited the formation of chondrogenic nodules and caused cell loss (Fig. 4A and C). The treatment increased the expression of *COL2A1* (Fig. 4D) and probably

Downloaded from http://hmg.oxfordjournals.org/ by guest on March 21, 2016

mutant *COL2A1*, which likely resulted in increased ER stress. This finding could explain the abnormalities observed in tissue morphogenesis during development and growth in the individuals with COL2pathy, because prochondrogenesis factors, including BMPs and TGFβs, necessarily presage the emergence of a specific developmental phenotype. During the development and growth of COL2pathy patients, prechondrogenic cells may initially adapt to the ER stress. However, when the chondrogenic cells mature in response to exposure to growth factors, including BMPs and TGFβs, the expression of *COL2A1* increases, increasing the ER stress beyond the limit of adaptation, triggering apoptotic signaling and the development of the disease phenotype. Thus, the ability of a cell to adapt to ER stress, and the nature of its adaptation strategies, can determine the disease phenotype.

Molecular chaperones can be a candidate therapeutic drug for COL2pathy

The adverse effects of BMP2 and TGFβ1 on the survival of COL2pathy-iChon cells suggest that the application of chondrogenic drugs will likely worsen the symptoms in patients with COL2pathy. However, we also discovered that chemical chaperones may be a promising treatment, because TMAO decreased the apoptosis of COL2pathy-iChon cells (Fig. 4E). TMAO is a natural chemical chaperone that directly acts on proteins in the unfolded state, thereby increasing the folding rate and stability of various mutant, otherwise labile, proteins (26). This function of TMAO led to improved secretion of type II collagen (Fig. 4F), decreasing ER stress in COL2pathy iChon cells (Fig. 4G and Supplementary Material, Fig. S4F) and differentiated COL2pathy iPS cells (Supplementary Material, Fig. S5D). It remains to be analyzed whether TMAO can rescue the folding of type II collagen in COL2pathy iChon cells. Additional studies will be needed to screen for more effective chemical chaperones that substantially rescue these cells from apoptosis that may be clinically applicable.

COL2pathy-iChon cells, chondrogenically differentiated COL2pathy-iPS cells and cartilage in teratomas from COL2pathy-iPS cells can be used complementarily

We detected abnormalities in COL2pathy-iChon cells as early as Day 14. This is a relatively short-term culture, and given them an advantage compared with iPS cells, which take several months to generate and subsequently redifferentiate into chondrocytes. Another advantage of this model is that a lot of iChon cell colonies can be obtained in each experiment. Time-lapse observations over the course of iChon cell induction showed that each iChon cell colony appears to be clonal (17,18), although it is possible that more than one cell may give rise to an iChon cell colony. Multiple colonies can be examined in iChon cell models, contributing to the reproducibility of the results. On the other hand, the abnormalities are exaggerated in iChon cell models. The formation of chondrogenic nodules from COL2pathy-iChon cells was severely reduced, whereas cartilage is still formed in COL2pathy patients, although to a lesser extent than healthy subjects. An advantage of using iPS cells is their ability to be expanded almost indefinitely, making it possible to use them for high-throughput drug screening.

We herein demonstrated that the cartilage in the teratomas generated from ACGII-iPS cells recapitulates the phenotypes seen in the cartilage of patients. The effects of candidate drug can be tested on human cartilage, by applying them to the mice harboring teratoma.

While useful for exploring pathologies that result from impaired protein trafficking, these cell-based models may have more limited utility when exploring pathologies that result from altered signaling between cells or between cells and matrix components. Matricellular signaling defects are emerging as an important pathogenic mechanism in skeletal diseases, and such defects are not well modeled in culture systems, because they do not yet recapitulate the complex structure of the mammalian growth plate and articular cartilages.

High-throughput screening, which requires a large number of cells may be performed using chondrogenically differentiated COL2Pathy-iPS cells. When the optimal category of therapeutic drug is determined (for example, molecular chaperone) and the numbers of compounds for screening are limited, the COL2pathy-iChon cells from fibroblasts can be used for the screening of these limited compounds. Such disease modeling by directed conversion of cells and iPS cells would also be useful for other skeletal dysplasias and cartilage diseases, and may have other applications for difficult to obtain tissues.

MATERIALS AND METHODS

Cell culture

COL2-pathy HDFs derived from four different patients (Supplementary Material, Table S1) were obtained from the cell banks of the Coriell Institute and Saitama Children's Medical Center. Control HDFs from two different neonates were purchased from KURABO (Strain #1439 and #789013). HDFs were cultured in DMEM (Sigma) with 10% FBS (Invitrogen), 50 U/ml penicillin and 50 μg/ml streptomycin. Human iChon cells were induced and maintained in DMEM (Sigma) with 10% FBS (Invitrogen), 50 U/ml penicillin and 50 μg/ml streptomycin. Human iPS cells were maintained in DMEM/F12 (Sigma) with 20% Knockout Serum Replacement (Invitrogen), 2 mM L-glutamine, 100 μM non-essential amino acids, 100 μM β-mercaptoethanol, 4 ng/ml bFGF (Wako), 50 U/ml penicillin and 50 μg/ml streptomycin on mitomycin-C-treated mouse embryonic fibroblasts.

Generation of iChon cells

Retroviral transduction was performed as described (17). Briefly, after nucleofection of the mouse *slc7a1* gene (Takahashi *et al.*, 2007), human fibroblasts were infected with retroviruses encoding c-MYC, KLF4 and SOX9 using Plat-E cells and the pMX system (Day 0). The next day, the infected fibroblasts (1×10^5 cells) were re-seeded into 100 mm dishes (Day 1), unless otherwise specified. In the case of iChon cell colony expansion, the infected fibroblasts (2×10^4 cells) were re-seeded into 100 mm dishes, and iChon cell colonies were picked up using 200 μl pipettes under a microscope, and were then re-seeded into the wells of a 24-well plate. The iChon cells were generated and maintained in DMEM supplemented with 10% FBS, unless otherwise specified. In the experiments shown in Figure 3, 50 μg/ml of ascorbic acid (Nacalai) or

Downloaded from http://hmg.oxfordjournals.org/ by guest on March 21, 2016

vehicle (water) was added to the medium from Day 6 to Day 17, and cells were subjected to an analysis on Day 17.

Alcian blue and toluidine blue staining

Cells were fixed in 100% methanol (Nacalai Tesque, Japan) for 2 min at −20°C, stained with pH 2.5 Alcian blue (Merck) or pH 4.1 toluidine blue (Wako) for 2 h at 25°C, and washed three times with distilled water. The Alcian blue- or toluidine blue-positive colony numbers were counted using the NIS Element software program (Nikon). We defined a colony as a cell cluster that was more than 0.5 mm in diameter.

Immunofluorescence

iChon cells were cultured on slides, fixed in 4% paraformaldehyde for 15 min at 25°C, washed three times with PBS and blocked for 18 h in PBS containing 0.3% BSA (Sigma) and 0.1% Triton X-100 (Nacalai) at 4°C. Primary antibodies against COL2A1 (Collagen II Ab-2, Thermo scientific), SSEA4 (ab16287, abcam) and TRA-1-60 (ab16288, abcam) in PBS containing 0.3% BSA and 0.1% Triton X-100 were applied for 1 h at 25°C. After washing the samples three times with PBS, secondary antibodies were applied for 1 h at 25°C.

RT–PCR and real-time RT–PCR analyses

The total RNA was extracted using RNeasy Mini Kits (Qiagen) or TRIzol (Invitrogen). The total RNAs prepared from the redifferentiated human primary fetal chondrocytes (HFC) were purchased from Cell Applications, Inc. (402RD-R10f). RT–PCR and real-time quantitative RT–PCR were performed as described previously (16). Briefly, 100 ng of total RNA was used to synthesize the first-strand cDNA (20 μl scale) that was used as a template (2 μl after 1:5 dilution) for RT–PCR and real-time RT–PCR. Real-time RT–PCR was performed in 384-well plates using the Step-One-Plus real-time PCR system (Applied Biosystem). Normalized expression levels were calculated using the comparative CT method, with the *GAPDH* mRNA expression level used as internal control. The primers used for real-time RT–PCR are listed in Supplementary Material, Table S3. Real-time RT–PCR was carried out with 'n' samples (each sample consisted of 10–20 iChon colonies) in Figures 1–4 and Supplementary Material, Figures S1, S2 and S4, or with one iPS clone tested in triplicate in Figures 5, 6 and Supplementary Material, Figures S5 and S7.

The primers used for the RT–PCR amplification of *COL2A1* cDNA fragments from ACGII-1 iChon cells (the experiment shown in Supplementary Material, Fig. S1B) are: forward, GAGAAGGGAGAAGTTGGACCTC and reverse, AGCCTC TCCTTTGTCACCTCTG. The primers used for the RT–PCR amplification of *XBP1* cDNA fragments from iChon cells (the experiments shown in Figs 2D and 3C) were: forward, AATG AAGTGAGGCCAGTGGCC and reverse, AATACCGCCAG AATCCATGGG.

TUNEL assay

iChon cell colonies were fixed in freshly prepared 4% paraformaldehyde for 1 h at 25°C. An *in situ* cell death detection kit (TMR red; Roche) was used according to the manufacturer's instructions. The ratio of TUNEL positive cells to the total cells in one iChon colony was calculated in this study. The numbers of colonies examined are indicated in the figure legends.

Antibodies and inhibitors

The primary antibodies against COL2A1 (Santa Cruz), phospho-eIF2a (Cell Signaling), ATF6 (abcam), GAPDH (Santa Cruz), and b-Actin (Cell Signaling) were applied for the western blot analyses using total cell extracts and supernatants prepared from iChon cell cultures. Alkaline phosphatase-conjugated secondary antibodies were purchased from Invitrogen. MG132 (Abcam) and bafilomycin A1 (Abcam) were used as the proteasome and lysosome inhibitors, respectively, as described in a previous report (27). We treated iChon cells with final concentration of 4 μM MG132 or 200 nM bafilomycin A1 for 18 h.

Western blot

Samples were subjected to electrophoresis in 3–8% Tris–Acetate gels (Invitrogen) in the absence of dithiothreitol and 2-mercaptethanol (under non-reducing condition) to detect type II collagen, and in gradient 4–12% Bis–Tris gels (Invitrogen) in the presence of 200 mM dithiothreitol after boiling for 5 min at 95°C to detect phospho-eIF2a and ATF6. The separated proteins were transferred to nitrocellulose membranes and incubated for 1 h at 25°C in 5% skim milk. The indicated primary antibodies (COL2A1 at a dilution of 1:200, phospho-eIF2a at 1:1000, ATF6 at 1:500, and GAPDH and β-Actin at 1:2000) were applied for 18 h at 4°C. After washing the samples three times with PBS, alkaline phosphatase-conjugated secondary antibodies (1:2000) were applied for 1 h at 25°C. After washing the membranes, the proteins were detected by the 4-nitro-blue-tetrazolium-chloride and 5-bromo-4-chloro-3-indolyl-phosphate reactions.

Preparation of TMAO

The stock TMAO (Tokyo chemical industry, Japan) solution was prepared by dissolving TMAO in distilled water at a concentration of 5 M. Aliquots of stock TMAO/water solutions were added to the culture medium. As a control, an equal amount of water was added to the medium. A total of 50 μg/ml ascorbic acid was added in addition to the medium in the experiment of Supplementary Material, Figure S4D.

Preparation of chondrogenic supplements

Chondrogenic supplementation was performed using 50 ng/ml BMP2 and 10 ng/ml TGFβ1 as a working concentration. Stock solutions of the chondrogenic supplements were prepared at ×1000 concentration in PBS containing 0.1% BSA, and were added to the culture medium. As a control, an equal volume of PBS containing 0.1% BSA was added to the medium.

Generation of human iPS cells and teratomas

Episomal plasmid vectors (Mixture Y4: *OCT3/4*, *SOX2*, *KLF4*, *L-MYC*, *LIN28*, and *p53* shRNA) were electroporated into

Downloaded from http://hmg.oxfordjournals.org/ by guest on March 21, 2016

human fibroblasts (28) with the Neon transfection system (Invitrogen). A week after transduction, 1×10^5 cells were re-seeded into 100 mm dishes with feeders. The cells were subsequently cultured in hiPS medium. To form teratomas, we injected 1×10^6 hiPS cells into the testicular capsules of BALB/c AJcl-*nu/nu* male mice. Then, 6–8 weeks later, tumors were cut into 5 mm pieces and fixed in 10% formalin. The tissue was embedded in paraffin and stained with hematoxylin and eosin.

In vitro chondrogenic differentiation of human iPS cells

Chondrogenic differentiation was performed following a previous report (23), with some modifications. To remove feeder cells, iPS cells were seeded and cultured in ReproFF2 (ReproCELL) medium on matrigel-coated dishes for two or three passages. After removing feeders (Day 0), the iPS cells were cultured in RPMI 1640 (Days 1–3) or DMEM (Days 4–14) supplemented with 1% FBS and human recombinant proteins (25 ng/ml WNT3A (R&D), 25 ng/ml Activin-A (R&D), 20 ng/ml FGF2 (R&D), 10 ng/ml TGFβ1 (Peprotech), 40 ng/ml BMP2 (Astellas, Japan) and 100 ng/ml GDF5 (PTT) (Supplementary Material, Fig. S5A). Differentiated cells were scraped on Day 14, and 5×10^5 cells were centrifuged at 500 g for 10 min in a 15 ml tube. Pellets were cultured in DMEM with 10% FBS, 50 μg/ml ascorbic acid, 10 ng/ml TGFβ1, 10^{-7} M dexamethasone, 100 μg/ml sodium pyruvate and ITS (10 μg/ml insulin, 5.5 μg/ml transferrin and 6.7 ng/ml sodium selenite) for 4 weeks (Days 14–42).

Immunohistochemical staining

Teratoma formation was induced using six control iPS and six ACGII iPS cell lines. Semi-serial histological sections generated from formalin-fixed teratomas were immunostained with the primary and secondary antibodies. For a positive control, sections obtained from the joint capsule of a knee from a rat were used to test the anti-type II antibodies (SBA-1320-01, BIOZOL).

Electron microscopy

Teratomas or iChon cells were fixed with 4% paraformaldehyde and 2% glutaraldehyde. Post-fixation was performed with 2% osmium tetroxide. In the case of the teratoma analysis, cartilage tissues were found according to the morphology of cells and toluidine blue staining. After dehydration, embedding and polymerization, ultrathin sections were stained with 2% uranyl acetate. They were observed with a HITACHI 7650 electron microscope at an acceleration voltage of 80 kV.

Statistical analysis

The data are shown as averages and standard deviations. In this study, we used two-tailed Student's *t*-tests or one-way ANOVA (analysis of variance) with a Tukey–Kramer *post-hoc* test for multiple comparisons. *P*-values <0.05 were considered to be statistically significant.

All experiments were approved by the institutional review board of Kyoto University and the institutional biosafety committee of Kyoto University.

SUPPLEMENTARY MATERIAL

Supplementary Material is available at HMG online.

ACKNOWLEDGEMENTS

We thank Nobuhiko Kan for providing samples. We thank Kaori Fujita and Hiromi Kishi for assistance.

FUNDING

This study was supported in part by the Japan Science Technology Agency (JST) (CREST to N.T.); Scientific Research Grants (24791541 and 26861187 to M.O., 24390354 to N.T.) from MEXT; the Research Center Network for Realization of Regenerative Medicine (to N.T.); and the Scientific Research from the Ministry of Health, Labor and Welfare of Japan (to H.S. and N.T.).

REFERENCES

1. Olsen, B.R., Reginato, A.M. and Wang, W. (2000) Bone development. *Annu. Rev. Cell Dev. Biol.*, **16**, 191–220.
2. Khoshnoodi, J., Cartailler, J.-P., Alvares, K., Veis, A. and Hudson, B.G. (2006) Molecular recognition in the assembly of collagens: terminal noncollagenous domains are key recognition modules in the formation of triple helical protomers. *J. Biol. Chem.*, **281**, 38117–38121.
3. Kielty, C.M., Hopkinson, I. and Grant, M.E. (1993) In Royce, P.M. and Steinmann, B. (eds), *Connective Tissue and its Heritable Disorders: Molecular, Genetic, and Medical Aspects*. Wiley-Liss, Inc., New York, pp. 103–147.
4. Warman, M.L., Cormier-Daire, V., Hall, C., Krakow, D., Lachman, R., LeMerrer, M., Mortier, G., Mundlos, S., Nishimura, G., Rimoin, D.L. *et al.* (2011) Nosology and classification of genetic skeletal disorders: 2010 revision. *Am. J. Med. Genet. Part A*, **155A**, 943–968.
5. Ala-Kokko, L., Baldwin, C.T., Moskowitz, R.W. and Prockop, D.J. (1990) Single base mutation in the type II procollagen gene (COL2A1) as a cause of primary osteoarthritis associated with a mild chondrodysplasia. *Proc. Natl Acad. Sci. USA*, **87**, 6565–6568.
6. Zankl, A., Zabel, B., Hilbert, K., Wildhardt, G., Cuenot, S., Xavier, B., Ha-Vinh, R., Bonafé, L., Spranger, J. and Superti-Furga, A. (2004) Spondyloperipheral dysplasia is caused by truncating mutations in the C-propeptide of COL2A1. *Am. J. Med. Genet. Part A*, **129A**, 144–148.
7. Bateman, J.F., Boot-Handford, R.P. and Lamandé, S.R. (2009) Genetic diseases of connective tissues: cellular and extracellular effects of ECM mutations. *Nat. Rev. Genet.*, **10**, 173–183.
8. Tsang, K.Y., Chan, D., Bateman, J.F. and Cheah, K.S.E. (2010) In vivo cellular adaptation to ER stress: survival strategies with double-edged consequences. *J. Cell Sci.*, **123**, 2145–2154.
9. Furuichi, T., Masuya, H., Murakami, T., Nishida, K., Nishimura, G., Suzuki, T., Imaizumi, K., Kudo, T., Ohkawa, K., Wakana, S. *et al.* (2011) ENU-induced missense mutation in the C-propeptide coding region of Col2a1 creates a mouse model of platyspondylic lethal skeletal dysplasia, Torrance type. *Mammalian Genome: Official Journal of the International Mammalian Genome Society*, **22**, 318–328.
10. Hintze, V., Steplewski, A., Ito, H., Jensen, D.a., Rodeck, U. and Fertala, A. (2008) Cells expressing partially unfolded R789C/p.R989C type II procollagen mutant associated with spondyloepiphyseal dysplasia undergo apoptosis. *Hum. Mutat.*, **29**, 841–851.
11. Aigner, T., Cook, J.L., Gerwin, N., Glasson, S.S., Laverty, S., Little, C.B., McIlwraith, W. and Kraus, V.B. (2010) Histopathology atlas of animal model systems - overview of guiding principles. *Osteoarth. Cartil.*, **18**(Suppl. 3), S2–S6.
12. Sun, N., Yazawa, M., Liu, J., Han, L., Sanchez-Freire, V., Abilez, O.J., Navarrete, E.G., Hu, S., Wang, L., Lee, A. *et al.* (2012) Patient-specific induced pluripotent stem cells as a model for familial dilated cardiomyopathy. *Sci. Translat. Med.*, **4**, 130ra147.

Downloaded from http://hmg.oxfordjournals.org/ by guest on March 21, 2016

13. Israel, M.a., Yuan, S.H., Bardy, C., Reyna, S.M., Mu, Y., Herrera, C., Hefferan, M.P., Van Gorp, S., Nazor, K.L., Boscolo, F.S. *et al.* (2012) Probing sporadic and familial Alzheimer's disease using induced pluripotent stem cells. *Nature*, **482**, 216–220.
14. Egawa, N., Kitaoka, S., Tsukita, K., Naitoh, M., Takahashi, K., Yamamoto, T., Adachi, F., Kondo, T., Okita, K., Asaka, I. *et al.* (2012) Drug screening for ALS using patient-specific induced pluripotent stem cells. *Sci. Translat. Med.*, **4**, 145ra104–145ra104.
15. Qiang, L., Fujita, R., Yamashita, T., Angulo, S., Rhinn, H., Rhee, D., Doege, C., Chau, L., Aubry, L., Vanti, W.B. *et al.* (2011) Directed conversion of Alzheimer's disease patient skin fibroblasts into functional neurons. *Cell*, **146**, 359–371.
16. Hiramatsu, K., Sasagawa, S., Outani, H., Nakagawa, K., Yoshikawa, H. and Tsumaki, N. (2011) Generation of hyaline cartilaginous tissue from mouse adult dermal fibroblast culture by defined factors. *J. Clin. Invest.*, **121**, 640–657.
17. Outani, H., Okada, M., Yamashita, A., Nakagawa, K., Yoshikawa, H. and Tsumaki, N. (2013) Direct induction of chondrogenic cells from human dermal fibroblast culture by defined factors. *PLoS ONE*, **8**, e77365.
18. Outani, H., Okada, M., Hiramatsu, K., Yoshikawa, H. and Tsumaki, N. (2011) Induction of chondrogenic cells from dermal fibroblast culture by defined factors does not involve a pluripotent state. *Biochem. Biophys. Res. Commun.*, **411**, 607–612.
19. Akiyama, H., Chaboissier, M.C., Martin, J.F., Schedl, A. and de Crombrugghe, B. (2002) The transcription factor Sox9 has essential roles in successive steps of the chondrocyte differentiation pathway and is required for expression of Sox5 and Sox6. *Genes Dev.*, **16**, 2813–2828.
20. Lefebvre, V., Li, P. and de Crombrugghe, B. (1998) A new long form of Sox5 (L-Sox5), Sox6 and Sox9 are coexpressed in chondrogenesis and cooperatively activate the type II collagen gene. *EMBO J.*, **17**, 5718–5733.
21. Smits, P., Li, P., Mandel, J., Zhang, Z., Deng, J.M., Behringer, R.R., de Crombrugghe, B. and Lefebvre, V. (2001) The transcription factors L-Sox5 and Sox6 are essential for cartilage formation. *Dev Cell*, **1**, 277–290.
22. Takahashi, K., Tanabe, K., Ohnuki, M., Narita, M., Ichisaka, T., Tomoda, K. and Yamanaka, S. (2007) Induction of pluripotent stem cells from adult human fibroblasts by defined factors. *Cell*, **131**, 861–872.
23. Oldershaw, R.A., Baxter, M.A., Lowe, E.T., Bates, N., Grady, L.M., Soncin, F., Brison, D.R., Hardingham, T.E. and Kimber, S.J. (2010) Directed differentiation of human embryonic stem cells toward chondrocytes. *Nat. Biotechnol.*, **28**, 1187–1194.
24. Lee, H.S., Doh, J.W., Kim, C.J. and Chi, J.G. (2000) Achondrogenesis type II (Langer-Saldino achondrogenesis): a case report. *J. Korean Med. Sci.*, **15**, 604–608.
25. Chan, D., Cole, W.G., Chow, C.W., Mundlos, S. and Bateman, J.F. (1995) A COL2A1 mutation in achondrogenesis type II results in the replacement of type II collagen by type I and III collagens in cartilage. *J. Biol. Chem.*, **270**, 1747–1753.
26. Bandyopadhyay, A., Saxena, K., Kasturia, N., Dalal, V., Bhatt, N., Rajkumar, A., Maity, S., Sengupta, S. and Chakraborty, K. (2012) Chemical chaperones assist intracellular folding to buffer mutational variations. *Nat. Chem. Biol.*, **8**, 238–245.
27. Ishida, Y., Yamamoto, A., Kitamura, A., Lamande, S.R., Yoshimori, T., Bateman, J.F., Kubota, H. and Nagata, K. (2009) Autophagic elimination of misfolded procollagen aggregates in the endoplasmic reticulum as a means of cell protection. *Mol. Biol. Cell*, **20**, 2744–2754.
28. Okita, K., Matsumura, Y., Sato, Y., Okada, A., Morizane, A., Okamoto, S., Hong, H., Nakagawa, M., Tanabe, K., Tezuka, K. *et al.* (2011) A more efficient method to generate integration-free human iPS cells. *Nat. Methods*, **8**, 409–412.

Downloaded from http://hmg.oxfordjournals.org/ by guest on March 21, 2016

Pediatr Radiol
DOI 10.1007/s00247-015-3518-2

ORIGINAL ARTICLE

Criteria for radiologic diagnosis of hypochondroplasia in neonates

Tomoko Saito[1] · Keisuke Nagasaki[1] · Gen Nishimura[2] · Masaki Wada[1] · Hiromi Nyuzuki[1] · Masaki Takagi[3,4] · Tomonobu Hasegawa[4] · Naoko Amano[4] · Jun Murotsuki[5] · Hideaki Sawai[6] · Takahiro Yamada[7] · Shuhei Sato[8] · Akihiko Saitoh[1]

Received: 26 February 2015 / Revised: 20 October 2015 / Accepted: 19 November 2015
© Springer-Verlag Berlin Heidelberg 2016

Abstract
Background A radiologic diagnosis of hypochondroplasia is hampered by the absence of age-dependent radiologic criteria, particularly in the neonatal period.
Objective To establish radiologic criteria and scoring system for identifying neonates with fibroblast growth factor receptor 3 (FGFR3)-associated hypochondroplasia.
Materials and methods This retrospective study included 7 hypochondroplastic neonates and 30 controls. All subjects underwent radiologic examination within 28 days after birth. We evaluated parameters reflecting the presence of (1) short ilia, (2) squared ilia, (3) short greater sciatic notch, (4) horizontal acetabula, (5) short femora, (6) broad femora, (7) metaphyseal flaring, (8) lumbosacral interpedicular distance narrowing and (9) ovoid radiolucency of the proximal femora.
Results Only parameters 1, 3, 4, 5 and 6 were statistically different between the two groups. Parameters 3, 5 and 6 did not overlap between the groups, while parameters 1 and 4 did. Based on these results, we propose a scoring system for hypochondroplasia. Two major criteria (parameters 3 and 6) were assigned scores of 2, whereas 4 minor criteria (parameters 1, 4, 5 and 9) were assigned scores of 1. All neonates with hypochondroplasia in our material scored ≥6.
Conclusion Our set of diagnostic radiologic criteria might be useful for early identification of hypochondroplastic neonates.

Keywords Achondroplasia · FGFR3 · Hypochondroplasia · Neonate · Radiography · Radiologic diagnosis · Scoring system

✉ Keisuke Nagasaki
nagasaki@med.niigata-u.ac.jp

[1] Division of Pediatrics,
Department of Homeostatic Regulation and Development,
Niigata University Graduate School of Medical and Dental Sciences,
1-757 Asahimachi-Dori, Chu-Ou-Ku,
Niigata 951-8510, Japan

[2] Department of Radiology,
Tokyo Metropolitan Children's Medical Center,
Tokyo, Japan

[3] Department of Endocrinology,
Tokyo Metropolitan Children's Medical Center,
Tokyo, Japan

[4] Department of Pediatrics,
Keio University School of Medicine,
Tokyo, Japan

[5] Department of Maternal and Fetal Medicine,
Tohoku University Graduate School of Medicine,
Miyagi Children's Hospital,
Sendai, Japan

[6] Departments of Obstetrics and Gynecology,
Hyogo College of Medicine,
Hyogo, Japan

[7] Departments of Obstetrics and Gynecology,
Hokkaido University Hospital,
Hokkaido, Japan

[8] Department of Obstetrics and Gynecology,
Aomori Rosai Hospital,
Aomori, Japan

Published online: 11 February 2016

Introduction

Hypochondroplasia is the mildest form of fibroblast growth factor receptor 3 (FGFR3)-associated skeletal dysplasia with an incidence of about 1 in 50,000 [1]. Affected individuals usually present after 2 years of age and seek medical help at preschool age because of mild body disproportion and short stature. A diagnosis of hypochondroplasia rests on the presence of several distinctive radiologic findings, such as broad long bones, lumbosacral interpedicular distance narrowing, short femoral necks and elongation of the fibula [2, 3]. However, the diagnosis of hypochondroplasia is hampered by the absence of age-dependent radiologic criteria, particularly in the neonatal period. It has been reported that younger affected children are not definitively diagnosed with hypochondroplasia [4].

We previously reported two cases of hypochondroplasia in children with FGFR3 mutations, focusing on prenatal ultrasonography findings in the third trimester and postnatal radiologic findings [5]. These children had short femora with increased biparietal diameter in utero; however, they were not diagnosed with hypochondroplasia in the neonatal period. The final diagnosis was made at the age of 3 years, when they visited our clinic because of short stature. Upon retrospective radiologic review, we learned that the radiologic findings relevant to hypochondroplasia were apparent in the neonatal period and that radiologic diagnosis may have been even easier in the neonatal period than in early childhood. The manifestations related to the ilia and proximal femora were particularly useful. The identification of short, squared ilia with short greater sciatic notches and horizontal acetabula along with the ovoid radiolucency of the proximal femora mimicking that of achondroplasia warranted the diagnosis.

The present study is dedicated to radiologic features in hypochondroplastic neonates with FGFR3 mutations and quantitative measurements that facilitate definitive diagnosis. We propose radiologic criteria for the identification of hypochondroplasia in the neonatal period.

Materials and methods

Subjects included seven hypochondroplasia neonates with FGFR3 mutations, three term neonates with nonsyndromic fetal growth restriction, and 30 term control subjects with available results of radiologic examination within 28 days after birth. All hypochondroplasia neonates underwent radiologic examination in the neonatal period, such as partial skeletal survey or chest and abdominal radiographs, because of short femoral length on fetal ultrasonography or clinically suspected disproportionate micromelia. Control subjects and individuals with nonsyndromic growth restriction were hospitalized from 2010 to 2014 and were born after 36 weeks of gestation. They did not have major congenital anomalies, and they underwent radiologic examination with extension position of hip joint and knee joint because of transient tachypnea of the newborn, meconium aspiration syndrome or suspected neonatal infection. We hypothesized that skeletal changes in the pelvic bones, femora and lumbar spine, which were seen in achondroplasia, were most useful for the diagnosis of hypochondroplasia. Accordingly, we calculated eight parameters and monitored one radiologic sign: (1) ratio of maximal transverse diameter of the ilia to its maximal longitudinal diameter (assessment of short ilia), (2) iliac angle (squared ilia), (3) length of the greater sciatic notches (short greater sciatic notch), (4) acetabular angle (horizontal acetabula), (5) ratio of femoral length (FL) to body length (femoral shortening), (6) ratio of diameter of the femoral mid-shaft to femoral length (broad femora), (7) ratio of width of the distal femoral metaphysis to femoral length (metaphyseal flaring), (8) ratio of interpedicular distance of the L1 vertebra to that of L4 (lumbosacral interpedicular distance narrowing) and (9) presence or absence of ovoid radiolucency of the proximal femora. Measurement procedures are illustrated in Fig. 1.

The open-source OsiriX software dedicated to the analysis of Digital Imaging and Communications in Medicine (DICOM) images (http://homepage.mac.com/rossetantoine/osirix) was

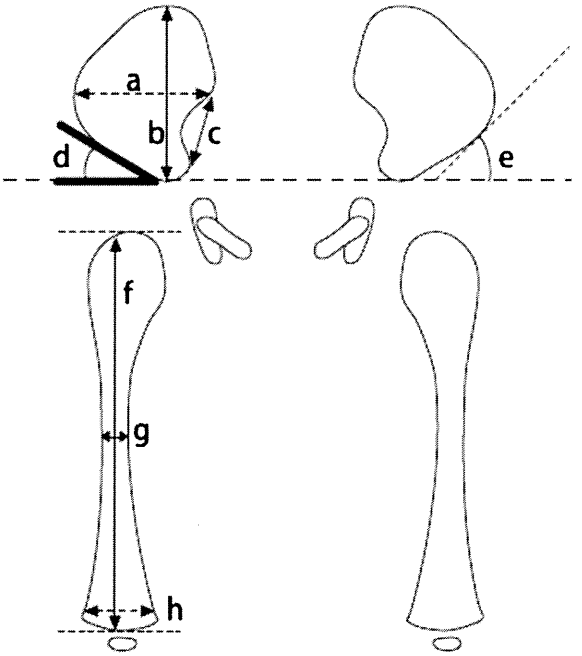

Fig. 1 Diagrams illustrate the measurements based on radiologic findings. The dotted line connects the bottom ends of the ilia: **a** maximal transverse iliac diameter, **b** maximal longitudinal iliac diameter, **c** greater sciatic notch, **d** acetabular roof angle, **e** iliac angle (formed by the tangent line of iliac wing with dotted line), **f** femur length, **g** mid-femur width, **h** maximal distal width of the femur

used for performing measurements. Only radiographs taken with the hip and knee joints extended and without significant joint rotation were analyzed.

Statistical significance of differences between control subjects and hypochondroplasia subjects was analyzed with the Mann–Whitney *U* test. A *P*-value < 0.01 was considered significant. All analyses were performed with JMP, version 10.0 (SAS Institute Inc., Cary, NC, USA).

This study was approved by the Institutional Review Board Committee at Niigata University School of Medicine, and informed consent was given by the parents or guardians of the patients with hypochondroplasia.

Results

Clinical manifestations of hypochondroplasia are summarized in Table 1. All the subjects with hypochondroplasia showed low femoral length and biparietal diameter at or above the higher limit of the normal range on prenatal ultrasonography. The results of the Shapiro-Wilk W test showed that all the measurement parameters in the control group followed the Gaussian distribution. The measurement parameters for short ilia, short greater sciatic notch, horizontal acetabula, short femora and broad femora (parameters 1, 3, 4, 5 and 6) were statistically different between the hypochondroplasia and control groups ($P < 0.01$), while the remaining parameters were not. Parameters 3, 5 and 6 did not overlap between the 2 groups, while parameters 1 and 4 did (Fig. 2). To distinguish subjects with hypochondroplasia from control subjects, we defined the following cut-off values based on the differences of at least 2 standard deviations from the average values in the control group: >0.80 for parameter 1, <7.5 mm for parameter 3, <22° for parameter 4, <0.14 for parameter 5 and >0.10 for parameter 6. Although assessment of ovoid radiolucency of the proximal femora was somewhat subjective, careful interpretation confirmed its presence in 6 out of 7 children with hypochondroplasia (Fig. 3). There were no abnormalities in other bones.

Based on these results, we defined a tentative scoring system for the diagnosis of hypochondroplasia (Fig. 4). The 2 major criteria (parameters 3 and 6 – short greater sciatic notch and broad femora) were assigned scores of 2. In addition, 4 minor criteria (parameters 1, 4, 5 and 9) were assigned scores of 1 for the following reasons: (a) femoral shortening (parameter 5) was a nonspecific finding; (b) short ilia and acetabular angle (parameters 1 and 4) showed overlaps between the hypochondroplasia neonates and normal controls and (c) the results of the assessment of ovoid radiolucency (parameter 9) were interpreter-dependent. Because all 7 neonates with hypochondroplasia showed combined scores of 6 points or more (Table 2), we presumed that a total score of 6 points or higher warrants thinking about a diagnosis of FGFR3-associated hypochondroplasia. We applied this scoring system to 30 control subjects and the 3 neonates with nonsyndromic growth restriction. The corresponding total scores were less than two in all these cases.

Discussion

It was previously believed that the diagnosis of hypochondroplasia was difficult to establish in infancy. However, recent in utero identification of short femora on prenatal ultrasonography has led to several reports on the early diagnosis of hypochondroplasia [6–10]. It has been found that discrepancy in growth between femoral length and biparietal diameter in the third trimester is highly indicative of this disease [5, 9, 11]. The final diagnosis of hypochondroplasia is established based on the molecular analysis of the FGFR3 gene. This test, however, is relatively expensive and a reliable radiology-based scoring system would be highly beneficial.

Table 1 Genetic and clinical manifestations in 7 children with hypochondroplasia

Child	1	2	3	4	5	6	7
FGFR3 mutation	L324V	N540K	N540K	N540K	S351C	N540K	N540K
Femur length standard deviation score in last trimester	−2.1	−2	-	−3.3	−3.3	−3.5	−2.7
Biparietal diameter standard deviation score in last trimester	0.3	1.3	-	3.3	0.3	3	1.8
Gestational age (weeks) at birth	38	40	38	38	39	38	39
Birth weight (g)	2,780	3,270	2,603	3,102	3,146	2,936	3,228
Birth length (cm)	45.5	49	44.5	49	47	46	45.5
Sex	M	M	F	F	M	F	M
Age at diagnosis[a]	3y 6 m	3y 6 m	1 m	2y	1y 7 m	1 m	1 m

M male, *F* female

[a] The diagnosis was based on the radiologic findings

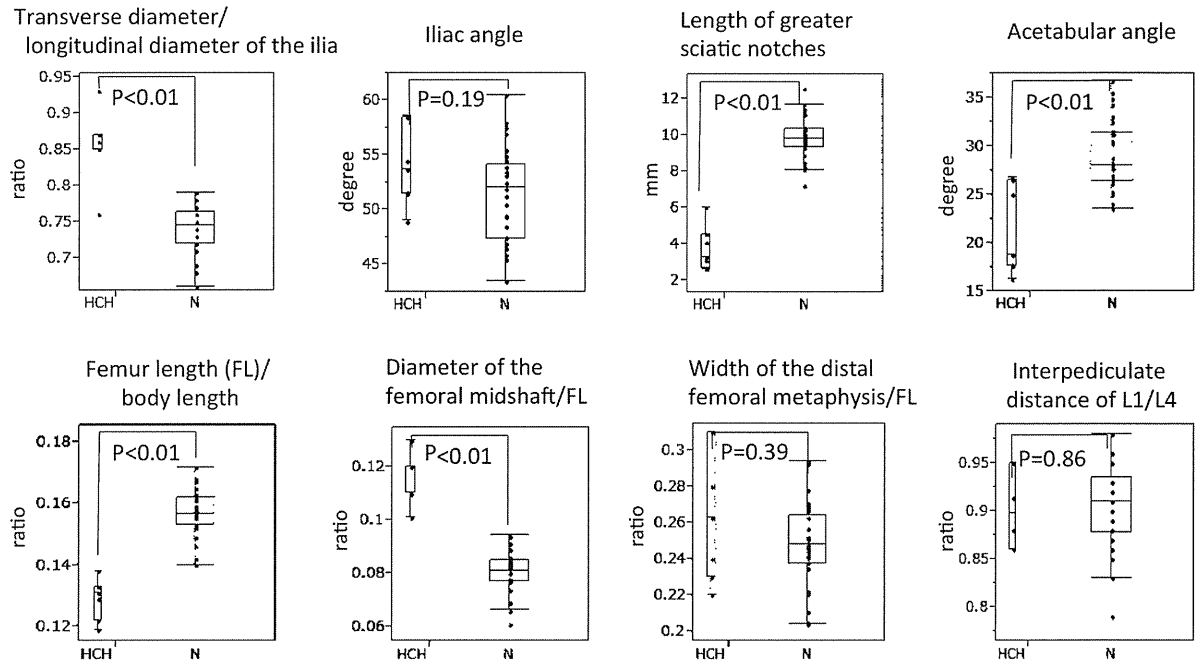

Fig. 2 Results of the measurements in 30 controls and in 7 children with hypochondroplasia. The bottoms and tops of the boxes correspond to the first and third quartiles, respectively, and the horizontal lines inside the boxes indicate the median values. Boxes show as follows: (1) Ratio of maximal transverse diameter to maximal longitudinal diameter of the ilia, (2) iliac angle, (3) length of the greater sciatic notches, (4) acetabular angle, (5) ratio of femoral length to body length, (6) ratio of diameter of the femoral mid-shaft to femoral length, (7) ratio of width of the distal femoral metaphysis to femoral length and (8) ratio of interpediculate distance of L1 to L4. Parameters 1, 3, 4, 5 and 6 were significantly different between the hypochondroplasia and control groups ($P < 0.01$). *HCH* hypochondroplasia, *N* control group

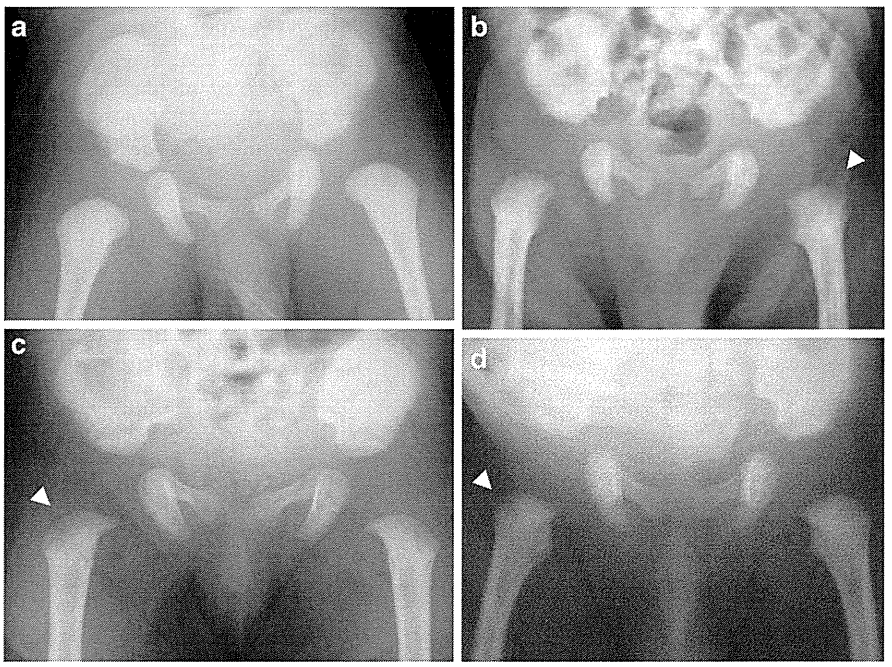

Fig. 3 Ovoid radiolucency of the femoral neck in anteroposterior radiographs. **a** A child in the control group; **b** Child 5 in the hypochondroplasia group (male neonate); **c** Child 6 in the hypochondroplasia group (female neonate); **d** Child 7 in the hypochondroplasia group (male neonate). An ovoid lucency (*arrowheads* in **b-d**) is seen in the femoral neck of the children with hypochodroplasia. All the subjects underwent radiologic examination in the neonatal period.

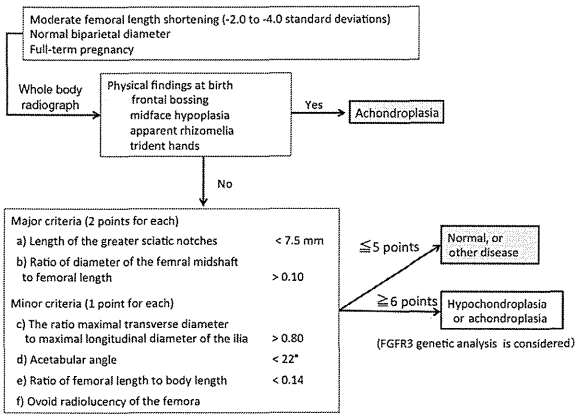

Fig. 4 Proposed flow chart for diagnosis of hypochondroplasia in the neonatal period

In this study, we used radiologic measurements of the ilia and femora to verify that hypochondroplastic neonates had short ilia with short greater sciatic notches and short, broad long bones. Furthermore, ovoid radiolucency of the proximal femora, which reflects the scooped-out appearance of the proximal femoral metaphysis typical of achondroplasia, was always discernible. Horizontal acetabula were also evident, but their presence was inconsistent among the hypochondroplasia neonates. In contrast, although lumbosacral interpedicular distance narrowing is an important diagnostic sign in childhood, it was not useful in our neonatal patients.

Identification of cases with mildly shortened femoral length has become more common with the widespread utilization of fetal ultrasonography. Such cases indicate the presence of mild bone dysplasia exemplified by hypochondroplasia, chromosome disorders such as trisomy 21, and nonsyndromic or syndromic fetal growth retardation (FGR). Although still tentative, our diagnostic criteria might be useful for the differentiation between hypochondroplasia and nonsyndromic growth restriction. Moreover, the radiologic changes in neonates with hypochondroplasia are relatively mild, and their identification may be difficult for nonexperts in bone dysplasias. This emphasizes the potential value of the measurement parameters proposed in the present study.

However, our scoring system is based on nonspecific skeletal changes, such as iliac hypoplasia, a scooped-out appearance of the proximal femora and short, broad femora; thus, it does not enable one to distinguish hypochondroplasia from other skeletal dysplasias, including mild achondroplasia [12]. The final radiologic diagnosis should depend on the overall pattern recognition and other distinctive skeletal changes. For example, cartilage hair hypoplasia causes a diagnostic difficulty in the neonatal period, as does hypochondroplasia [13]. However, mild femoral bowing and round distal femoral epiphyseal ossification warrant a diagnosis of cartilage hair hypoplasia. Molecular diagnoses are essential in difficult cases. To be essential, our scoring system would be utilized as screening for mild neonatal skeletal dysplasias.

The relatively small number of subjects is also a limitation of this study. Furthermore, all measurements were obtained in term neonates; it is currently unknown whether these data are applicable to premature neonates. Finally, correct positioning (extended hip and knee joints without joint rotation) is essential for obtaining interpretable measurements. Further studies in a larger population of hypochondroplasia, including premature neonates, are warranted to validate these criteria for the diagnosis of hypochondroplasia.

Conclusion

We propose a set of diagnostic radiologic criteria that can be useful for early identification of hypochondroplastic neonates.

Table 2 Application of the new scoring system to 7 neonates with hypochondroplasia

Parameter	Child	1	2	3	4	5	6	7
3	Short greater sciatic notches	2	2	2	2	2	2	2
6	Broad femora	2	2	2	2	2	2	2
1	Short ilia	1	1	1	1	1	1	0
4	Horizontal acetabula	1	1	0	1	0	1	0
5	Femoral shortening	1	1	1	1	1	1	1
9	Ovoid radiolucency of the femoral neck	1	0	1	1	1	1	1
Total score		8/8	7/8	7/8	8/8	7/8	8/8	6/8

Acknowledgments We would like to thank the following associates for their assistance with this study: Norio Shinozuka, MD, Akinori Taguchi, MD, Hidenori Haruna MD, and Kaoru Obinata, MD. This study was supported by the NNPL Growth Hormone Award 2010 and a grant-in-aid for Scientific Research from the Ministry of Health, Labour and Welfare of Japan, H26-Nanchitou (Nan)-Ippan-055.

Compliance with ethical standards

Conflict of interest None